

Hydrologic soil group based curve number matrix modeling for Enset-Based land use system in Meki River Watershed, Western Lake Ziway Sub-Basin, Central Rift Valley of Ethiopia

Alemu Beyene Woldesenbet (✉ alemu.beyene@aau.edu.et)

Addis Ababa University

Sebsebe Demisew Wudmatas

Addis Ababa University

Mekuria Argaw Denboba

Addis Ababa University

Azage Gebreyohannes Gebremariam

Addis Ababa University

Research

Keywords: Enset, CN, SCS, Infiltration, Carbon stock, HSG, HEC-HMS

Posted Date: January 5th, 2021

DOI: <https://doi.org/10.21203/rs.3.rs-136585/v1>

License: © ⓘ This work is licensed under a Creative Commons Attribution 4.0 International License.

[Read Full License](#)

1 **Hydrologic soil group based curve number matrix modeling for Enset-Based land**
2 **use system in Meki River Watershed, Western Lake Ziway Sub-Basin, Central**
3 **Rift Valley of Ethiopia**

4 Alemu Beyene Woldesenbet ¹, Sebsebe Demisew Wudmatas ², Mekuria Argaw Denboba ³, Azage
5 Gebreyohannes Gebremariam ⁴

- 6 1. Departments of Water Resources Engineering and Management, Ethiopian Institute of Water
7 Resources, Addis Ababa University, Ethiopia and Departments of Hydraulic and Water resources
8 Engineering, Wolkite University, Ethiopia (The corresponding author)
9 (alemu.beyene@aau.edu.et; Mob. 0911921985)
- 10 2. Departments of Plant Biology and Biodiversity Management, College of Natural and
11 Computational Sciences, Addis Ababa University, Ethiopia
- 12 3. Centers for Environmental Sciences, College of Natural and Computational Sciences, Addis
13 Ababa University, Ethiopia
- 14 4. Departments of Water Resources Engineering and Management, Ethiopian Institute of Water
15 Resources, Addis Ababa University, Ethiopia

16 This article can be cited as:

17 "Alemu Beyene, Sebsebe Demisew, Mekuria Argaw, Azage Gebreyohannes (2020). Hydrologic soil group based curve number
18 matrix modeling for Enset-Based land use system in Meki River Watershed, Western Lake Ziway Sub-Basin, Central Rift Valley of
19 Ethiopia, International Journal of Environmental Systems Research, Springer open."
20

Abstract

22 **Background**

23 *Enset-Based land use system (EBLUS) exhibits good carbon stock and infiltration rate equivalent*
24 *to forest covered areas, which enhances infiltration and water holding capacity and it can*
25 *reduce the curve number (CN) of the watersheds but it was not considered in former studies.*
26 *Therefore, this study is planned to model the hydrologic soil group (HSG) based CN matrix of*
27 *EBLUS relative to other LUSs with established hydrological characteristics in the Meki river*
28 *watershed. The soil data is used to determine the HSG of the watershed collected from Ministry*
29 *of Water, Irrigation and Energy (MOWIE) and verified by Harmonized World Soil Database*
30 *(HWSD). A Model is developed for CN of EBLUS relative to other LUSs (Alemu's formula). The*
31 *model considers both infiltration rate measured using Amozimeter and carbon stock of soil*
32 *weighed as 85% and 15% respectively. HEC-GEO-HMS model is used to consider the CN of EBLUS*
33 *as a separate LUS to verify the developed CN matrix model to generate CN of the sub-*
34 *watersheds.*

35 **Result**

36 *The field measurement results show that an infiltration rate of 12.9675,11.1875,10.375,7.065*
37 *and 12.8125mm hr⁻¹ for Natural Forest, Grassland and plantation, cultivated, built-up and*
38 *EBLUS respectively. The model is: $E = \frac{0.85 * \sum_{i=1}^n ELi + 0.15 * \sum_{i=1}^n ECsi}{n}$ and the resulting CN matrix of*
39 *EBLUS is 39,51.5,58.3 and 61.6 for HSG of A,B,C and D respectively.*

40 **Conclusion**

41 *Significant reduction in mean CN of the watershed that shows the role of EBLUS in managing*
42 *the water resources and flood is high. Therefore, escalating EBLUS will reduce the CN of the*
43 *watershed which reduces runoff volume in the watershed and it ensures the sustainability of*
44 *Lake Ziway by reducing sedimentation.*

45 **Key words:** *Enset, CN, SCS, Infiltration, Carbon stock, HSG, HEC-HMS*

46

47

1. Introduction

48 Land use and land cover (LULC) changes affect the processes that provide redistribution of soil
49 material and soil properties (Jerzy, Anna, & Jan, 2014) and it leads to change in soil organic
50 carbon (SOC) and soil quality (Nyssen, Habtamu, Mulugeta, Amanuel, Nigussie, & Mitiku, 2008).
51 Soil infiltration capacities are spatially and temporally dynamic properties due to varying land
52 use management practices (Oliver, Niels, Hogler, & Reinhard, 2006).

53 Land cover affects the infiltration capacity of the soil (A., B., & J., 2011; Schilling, Jha, Zhang,
54 Gassman, & Wolter, 2008; Mao & Cherkauer, 2009; Elfert & Bormann, 2010; Ghaffari, Keesstra,
55 Ghodousi, & Ahmadi, 2010), surface and subsurface flow regimes (base flow) (A., B., & J., 2011;
56 Tu, 2009), surface roughness (A., B., & J., 2011; Feddema, et al., 2005) and peak runoff (A., B., &
57 J., 2011; Burch, Bath, Moore, & O'Loughlin, 1987) and flood frequency and magnitude (A., B., &
58 J., 2011; Ward, Renssen, Aerts, van Balen, & Vandenberghe, 2008; Remo, Pinter, & Heine;
59 Benito, Rico, Sanchez-Moya, Sopeña, THorndycraft, & Barriendos, 2010; Qiu, Jia, Zhao, Wang,
60 Bennett, & Zhou, 2010).

61 Similarly, based on Kebede Wolka *et al.*, (2015), Enset-Based land use systems (EBLUS) can
62 reduce the rain drop impact equivalent to the forest and it exhibited a good carbon stock
63 equivalent to high-vegetation areas (Mesfin, Osamu, Christine, & Kumelachew, 2017; Mbow,
64 Van Noordwijk, Luedeling, Neufeldt, Minang, & Kowero, 2014) that modifies the infiltration and
65 water holding capacity of the soil for a longer period (Barbora & Jaroslava, 2014) which in turn
66 influences the curve number (CN) of Meki river watershed.

67 The socio-economic (Shiferaw Feleke, 2003), yield and inputs required (Uloro & Mengel, 2014),
68 EBLUS as a food security tool and as a sources of income (Mesfin, Osamu, Christine, &
69 Kumelachew, 2017; Mbow, Van Noordwijk, Luedeling, Neufeldt, Minang, & Kowero, 2014;
70 Tilahun & Robert, 2006; Anita, et al., 1996), the physiological (Admasu Tsegaye 1 and
71 P.C.Struik2, 2003), ecosystem services (Mesfin, Osamu, Christine, & Kumelachew, 2017),
72 agronomy (Admasu, 2007), breeding (James Harrison 1, 2014), pathology (Bridge, 1992),
73 postharvest (Yirmaga, 2013) and soil nutrition (Elias, 2011) aspect of EBLUS are studied.

74 The Relative impact of EBLUS on surface water has not been established and quantified (Anita,
75 et al., 1996; Uloro & Mengel, 2014) and the impact of EBLUS changes on hydrological processes
76 are not fully understood (A., B., & J., 2011; Wang, Liu, Kubota, & Chen, 2007) and contribution
77 of EBLUS to modify the CN responsible to model peak runoff (Merwade V., 2012) is not studied
78 formerly in the Meki river watershed.

79 Considering the importance of Meki river watershed and its role in contributing to the
80 sustainability of lake Ziway, detailed watershed modeling and analysis are needed including an
81 assessment of how the change in EBLUS at different scales (e.g., from the hydrologic response
82 unit to the basin scale) influenced the CN in the watershed to understand the underlying
83 mechanisms and to establish theory regarding the effects of EBLUS on CN of Meki river
84 watershed.

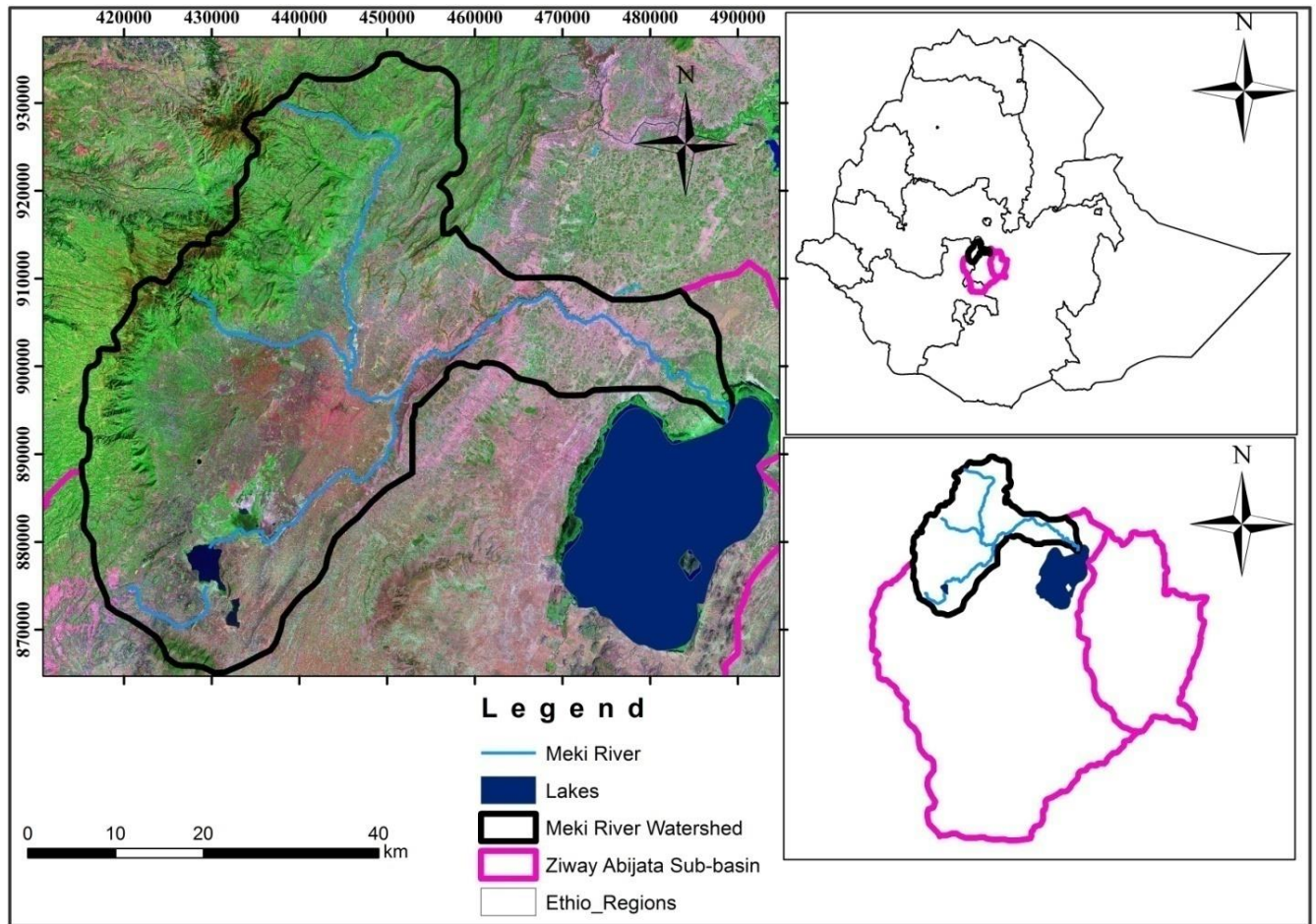
85 Therefore, the aim of this study is to articulate the influence of Enset-Based land use system
86 (EBLUS) on Curve number (CN) and to develop a model for HSG based CN matrix of EBLUS

87 relative to other land use systems with established hydrological characteristics in Meki river
88 watershed.

89 **2. Methods**

90 **2.1. Study area description**

91 Meki river watershed is found in the western part of lake Ziway between 7⁰45'N to 8⁰30'N and
92 38⁰10'E to 39⁰00'E as shown in Figure 1 in the Central Rift Valley (CRV) of Ethiopia and the
93 watershed has a mean elevation of 2169m.a.s.l, the mean annual rainfall ranges from 824mm
94 to 1292mm and the mean monthly temperature varies between 15°C and 29°C, the mean
95 relative humidity of 60%, average wind speed of 1.66m/s and average sunshine hour of 7.3 hrs
96 (Alemu Beyene *et al*, 2020; ENMA, 2017; Oliver et al., 2007).



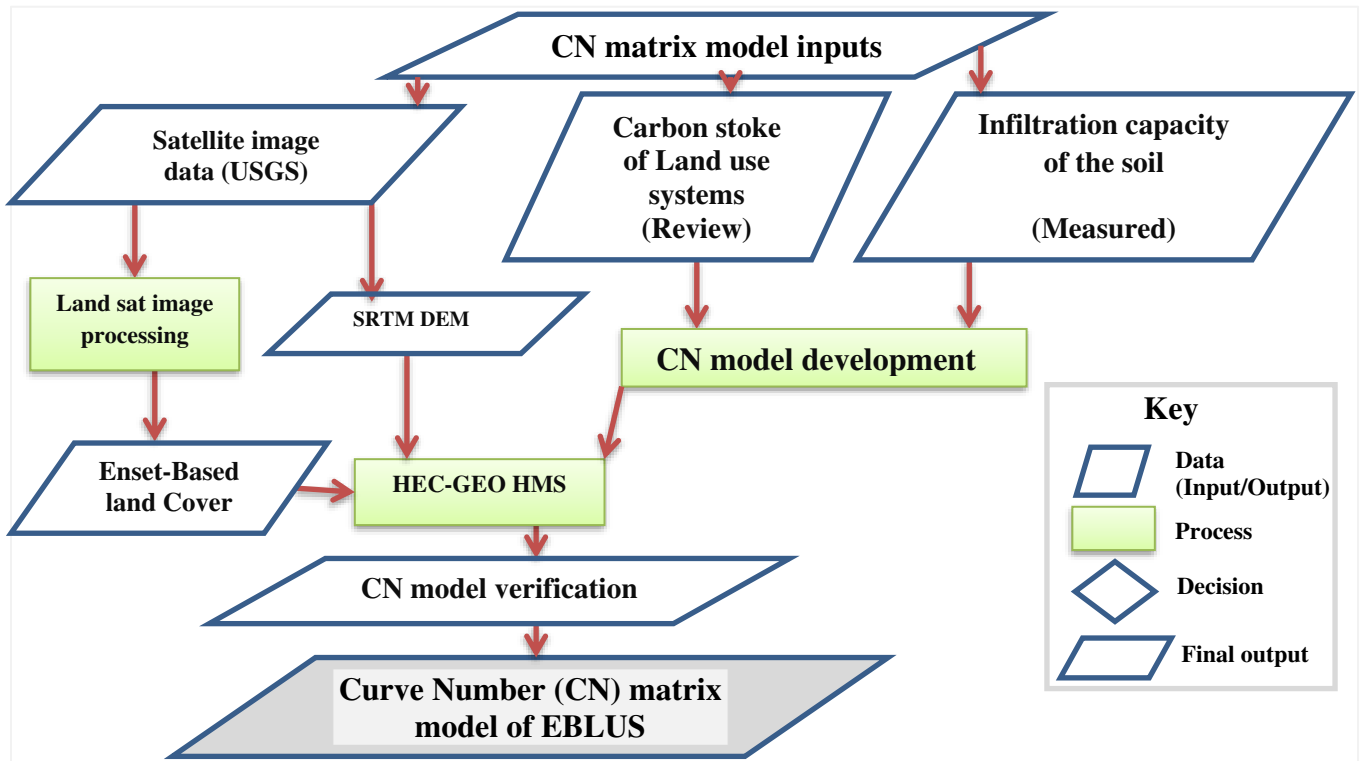
98 Figure 1: Study area map

99 **2.2. Research Framework**

100 Soil organic carbon and Land use are the critical factors to influence the infiltration capacity of
 101 the soil (Yimer, 2008; A.O.Ibeje, 2018). The mean steady state infiltration rates of farmlands,
 102 bamboo fields and forestland are 1.98 cm/h, 2.44cm/h and 2.43cm/h respectively (A.O.Ibeje,
 103 2018). This shows that the infiltration rate of the soil is under the influence of land use and also
 104 the land use change can affect the infiltration capacity of the soil (A.O.Ibeje, 2018).

105 Enset-Based land use system (EBLUS) considered in the land cover classification process using
 106 ERDAS imagine software with maximum likelihood algorithm and used to model the CN matrix

107 of Meki river watershed. Therefore, this study articulates the influence of EBLUS on CN of Meki
 108 river watershed and model the CN matrix for EBLUS as shown in the Flow diagram presented in
 109 Figure 2.

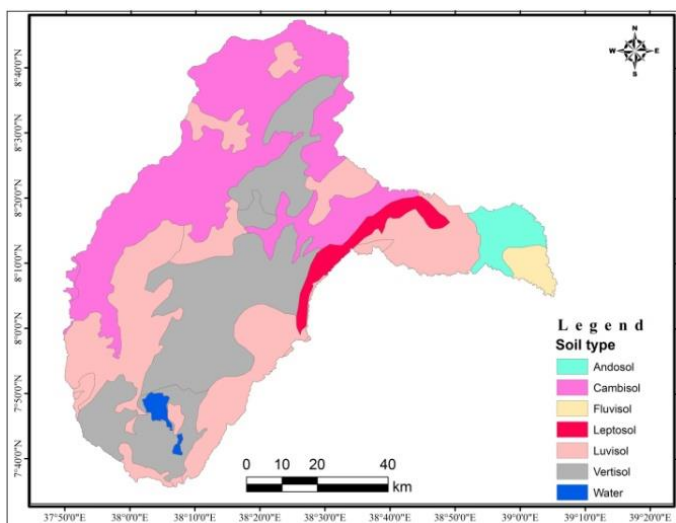
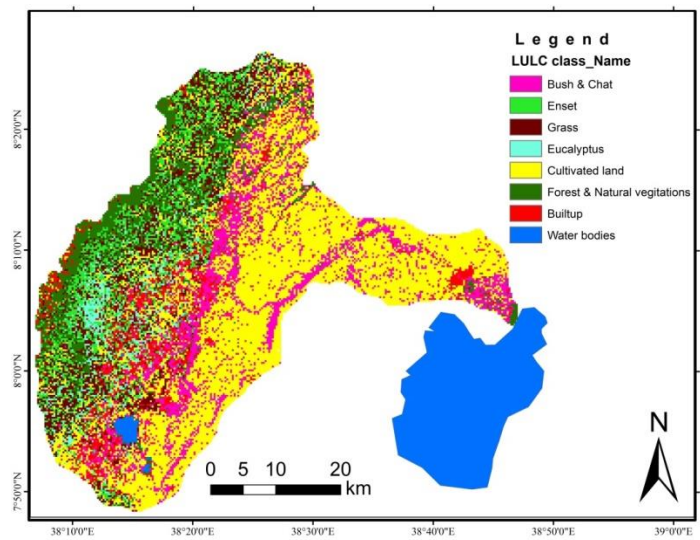
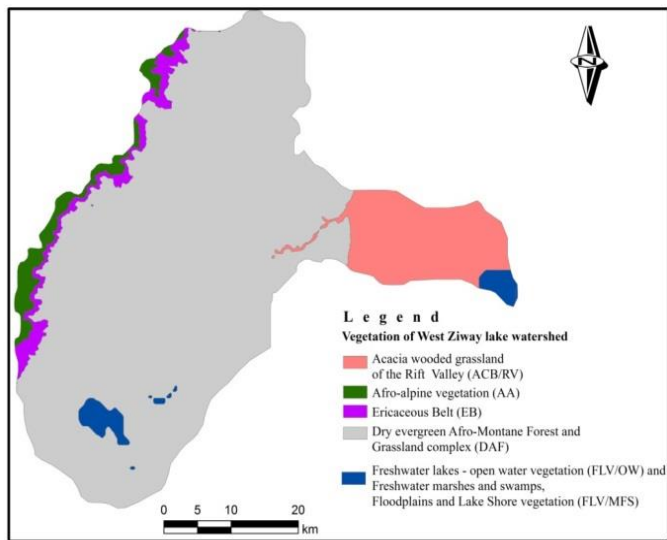


110
 111 Figure 2: CN matrix model flow diagram

112 2.3. Field measurement and analysis of infiltration capacity of LUS

113 Sample site selection criteria

114 Measuring and mapping of vegetation zone based infiltration rate of the soil under different
 115 land use systems to evaluate their relative hydrological influence are achieved using Amozimeter
 116 in the labor intensive field work. The soil type (soil texture) is one of the bases for sample
 117 site selection next to vegetation zone.



118 Figure 3: Dominant Vegetation zone, Land cover & soil type maps of the study area

119 Preliminary GPS based site assessment was carried out starting from the highest point of the
 120 watershed to Lake Ziway which is characterized by high elevation differences from 1633m.a.s.l
 121 at the gauging station of Meki river discharge to 3612m.a.s.l at Zebidar Mountain which can
 122 give enough head and opportunity for water resources development options.

123 In the process of field measurement site selection; Vegetation zone, dominant LUS and
124 Dominant soil types in the study area as shown in Figure 3 are considered as the main factors
125 influencing the infiltration capacity of the soil and the sampling matrix is prepared after the
126 overlay of those maps together so as to choose appropriate locations to organize the proposed
127 field measurement.

128 **Sampling and Measurement techniques**

129 In order to get and compare the hydrological characteristics of EBLUS, the following sampling
130 matrix was prepared as shown in Table 1. In the process of sampling, land use class is crucial for
131 the relative comparison of hydrological components (infiltration capacity) with replication.

132 The study area is classified in to eight land cover classes that include forest and natural
133 vegetation LUS, grass LUS, EBLUS, eucalyptus with sparse vegetation LUS, cultivated LUS, built-
134 up and degraded LUS but due to non-availability of data for all eight LUSs and for the ease of
135 sampling, the LUSs are aggregated as Cultivated LUS, Built-up & Degraded LUS, Grass &
136 Plantation LUS, EBLUS and Natural Forest LUS for the sampling purposes. The soil type data is
137 collected from MOWIE GIS section and Vertisol, Cambisol, Luvisol and Leptosol are considered
138 as the dominant four soil types in the watershed. The soil type is verified by harmonized world
139 soil database (HWSD).

140 The vegetation zones are combined with dominant soil types as vegetation zone 1 with soil type
141 1 (Z11) up to vegetation zone 3 with soil type 4 (Z34). Vegetation zones are expressed as Afro-
142 alpine as vegetation zone 1, Dry Afro-montane as vegetation zone 2 and Acacia wooded grass

143 land of rift valley as vegetation zone 3 verified in the field as shown in Figure 4 below and the
144 dominant soil types considered are Vertisol, Cambisol, Luvisol and Leptosol and called to be soil
145 type 1, soil type 2, soil type 3 and soil type 4 respectively as shown in Table 1.



146

147 Figure 4: Vegetation zone verification assessment

148 A = Divide line at western end of the watershed where more than half part of the watershed is
149 visible (Silti zone)

150 B & F = Western upper part of Meskan woreda (Yewutin & Yetebon respectively)

151 C = Found around Eastern Meskan woreda and Western Sodo woreda

152 D = Scene at Chohamba Meskan woreda

153 E = Conversion from lake to wetland (Lake Ziway)

Table 1: Sampling points based on vegetation zone, Dominant soil type and Dominant LUS

		Land Cover				
		Cultivated LUS	Builtup& Degraded LUS	Grass & Planted Forest LUS	EBLUS	Natural Forest LUS
Combined Vegetation & Dominant Soil type class 1	Z11	CZ11	BZ11	GZ11	EZ11	NZ11
	Z12	CZ12	BZ12	GZ12	EZ12	NZ12
	Z13	CZ13	BZ13	GZ13	EZ13	NZ13
	Z14	CZ14	BZ14	GZ14	EZ14	NZ14
	Z21	CZ21	BZ21	GZ21	EZ21	NZ21
	Z22	CZ22	BZ22	GZ22	EZ22	NZ22
	Z23	CZ23	BZ23	GZ23	EZ23	NZ23
	Z24	CZ24	BZ24	GZ24	EZ24	NZ24
	Z31	CZ31	BZ31	GZ31	EZ31	NZ31
	Z32	CZ32	BZ32	GZ32	EZ32	NZ32
	Z33	CZ33	BZ33	GZ33	EZ33	NZ33
	Z34	CZ34	BZ34	GZ34	EZ34	NZ34

There are about 60 sampling possibilities, but EBLUS is not common at the acacia wooded part of the watershed for which zones Z31 to Z34 to all LUSs are not applicable in this research.

The resulting sampling points are Z11 up to Z24 (8 combined zones of two vegetation zones and four dominant soil types) for five LUSs which results in 40 sampling points replicated to four fold to make it representative and to reduce human and instrumental errors.

¹ CZ23 refers to Cultivated LUS in vegetation zone two (Dry afro-montane) and soil type three (Luvisol)

The infiltration data collected from those sampling points using Amozimeter as shown in Figure 5. Hence, 160 samples were collected in the field excluding the lower zone of the watershed since it has no sufficient EBLUS to be considered and the result is analyzed and mapped using ArcGIS 10.1 for their hydrological characteristics of different land use systems compared with EBLUS.

Enset-Based land use system (EBLUS) was not included in all former land use studies and now in this portion more focus is deputed to the infiltration capacity of EBLUS relative to all land use systems in Meki river watershed. Amozimeter is used to measure the infiltration capacity of soil under each land use system, including EBLUS as shown in Figure 5 and considered to model CN matrix of EBLUS.



Figure 5: Amozimeter infiltration measurement of EBLUS

The hole dug to the level to which the water is released into the ground through sensor at the tip of the plastic pipe attached to the main tanker of the Amozimeter. The level of digging the

hole depends on the number of pipes filled to keep the balance pressure which is equivalent to 0.5m deep for one pipe. The main tanker was filled from the top with clean water to protect blockage of flowing pipes of the instrument to the sensor.

The water is released to flow down to the ground and time and depth of flow recorded using a stopwatch and gauge fitted to the instrument respectively based on the procedural manual.

2.4. Review of Carbon stock of Land use systems

Published articles are reviewed to get the carbon stock of different land use systems which accounts EBLUS. According to Mesfin *et al*, 2017, carbon stock of land uses are measured and reported as shown in Table 2 and considered to develop the CN of EBLUS.

Table 2: Carbon stock of different land use systems (Source: Mesfin *et al*, 2017)

Land Cover/Land Use	Carbon stock (ton/yr)
Open Water	0
Built-up, Medium Intensity LUS	132
Natural Forest LUS	45,714
Grasslands (Pasture) & plantations LUS	8350
Cultivated LUS	19,950
Enset-Based LUS	77,286

2.5. Review of HSG based curve number of land use systems

CN matrix is developed for all land use systems except EBLUS as shown in Table 3 that is used to develop a relation among the model the CN matrix for EBLUS relative to other land use systems with predetermined CN.

Table 3: Curve number lookup table (ERA, 2013; Chow, 1988)

Land Cover/Land Use	Hydrologic Soil Group			
	A	B	C	D
Open Water	100	100	100	100
Developed, Open Space	39	61	74	80
Developed, Low Intensity	57	72	81	86
Developed, Medium Intensity	77	85	90	92
Developed, High Intensity	98	98	98	98
Barren Land, Rock, Sand, Clay	63	77	85	88
Deciduous Forest	36	60	73	79
Evergreen Forest	36	60	73	79
Mixed Forest	36	60	73	79
Scrub/Shrub	35	56	70	77
Grasslands, Herbaceous	39	61	74	80
Pasture, Hay	49	69	79	84
Cultivated Crops	67	78	85	89
Woody Wetlands	100	100	100	100
Emergent Herbaceous Wetlands	100	100	100	100

The CN matrix of the dominant land use systems are used in modeling the CN matrix of EBLUS in Meki river watershed.

2.6. CN Matrix Model development method

The formerly developed CN matrix for all land use systems (LUSs) except EBLUS, infiltration capacity of the soil under all LUSs including EBLUS and carbon stock of the soil under all LUSs including EBLUS are used to develop a model for CN matrix of EBLUS relative to other LUSs with predetermined CN using Microsoft excel.

2.7. Preprocessing and CN model verification procedure in HEC-GeoHMS

Soil conservation service curve number grid is used by many hydrologic models to extract the curve number for watersheds (Fleming & Brauer, 2018; Merwade, 2012) for further analysis of watershed parameters and runoff modeling. To produce the CN grid several activities are expected that include watershed delineation, land use grid preparation, HSG grid preparation, merge the land use and soil data, create CN lookup table and finally creating the CN grid for Meki river watershed.

1.1.1. Delineation of the watershed from DEM

Meki river watershed and sub-watersheds are automatically extracted from Digital Elevation Model (DEM) and the DEM is preprocessed to produce the watershed fill, flow direction, flow accumulation, stream definition, stream segmentation, combined stream link, sink link, catchment grid delineation, catchment polygon processing, flow length, slope, Elevation, aspect, contour line, drainage line processing and adjoinment catchment processing, etc are derived using HEC-GeoHMS model of Arc GIS 10.1(Iliasse Khaddor & Adil HafidiAlaoui, 2014).

The project setup is generated using the outlet point at Lake Ziway by providing the data at the preprocessing phase of the project. Basin merge and river merge processes are taken place to increase consistency and convenience of the result output.

According to Fleming and Brauer (2018), in order to perform CN modeling, various types of information are required that includes watershed parameters from DEM, HSG and LUSs and the CN grid is used by many hydrologic models (Merwade, 2012).

1.1.2. Land use data preparation for CN grid

Land use map was generated using Land sat image data (30m) supported by Google earth. GPS based field visit is performed to collect data to train ERDAS 2014 to classify the images with maximum likelihood clustering algorithm of supervised classification method (Iliasse and Adil , 2014; Fleming and Brauer 2018) and eight Land use systems are identified as shown in

Figure 6 and reclassified into five classes as shown in According to Fleming and Brauer (2018) and Merwade (2012), the Spatial Analyst Tools in Arc Toolbox is used to implement re-classification

Table 4 based on the USGS land cover institute (LCI²) and modified to include the recently recognized EBLUS (Fleming and Brauer, 2018; Okirya Martin, Albert Rugumayo and Janka Ovcharovichova, 2012; Merwade, 2012).

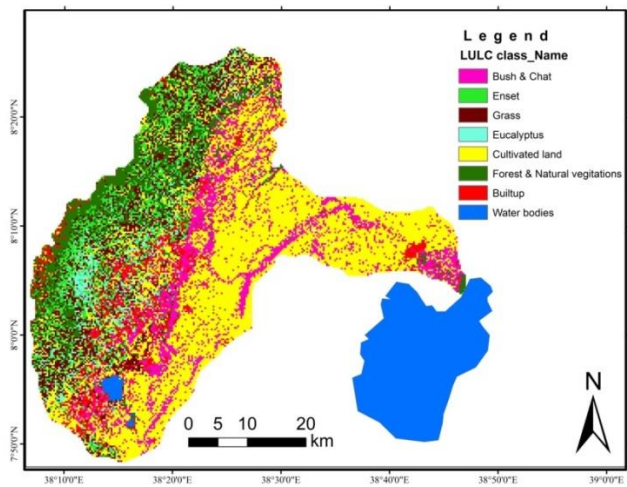


Figure 6: Land use system of the area for CN mapping

According to Fleming and Brauer (2018) and Merwade (2012), the Spatial Analyst Tools in Arc Toolbox is used to implement re-classification

² <http://landcover.usgs.gov/classes.php>

Table 4: Land use reclassification based on USGS land cover institute (LCI) with modification

Land cover classification		Revised classification	
Number	Description	Number	Description
11	Water bodies	1	Water
95	Wetlands with herbaceous plants		
21	Developed, Open space LUS	2	Built ups
22	Developed, Low and medium intensity LUS		
23	Developed, High intensity LUS		
43	Mixed forest LUS	3	Forest& Natural vegetation
42	Natural forest LUS		
41	Plantation LUS		
31	Bare land LUS	4or 5	Agricultural

82	Cultivated land LUS		
52	Grass land LUS		
	Enset	6	EBLUS

In the reclassification window, confirm the Input raster is LULC_2017_March2019Recl field is Class_Name, and then manually assign the new numbers from Table 4 as shown in Figure 7 and the output raster is saved as LULC_2017_March2019Recl.

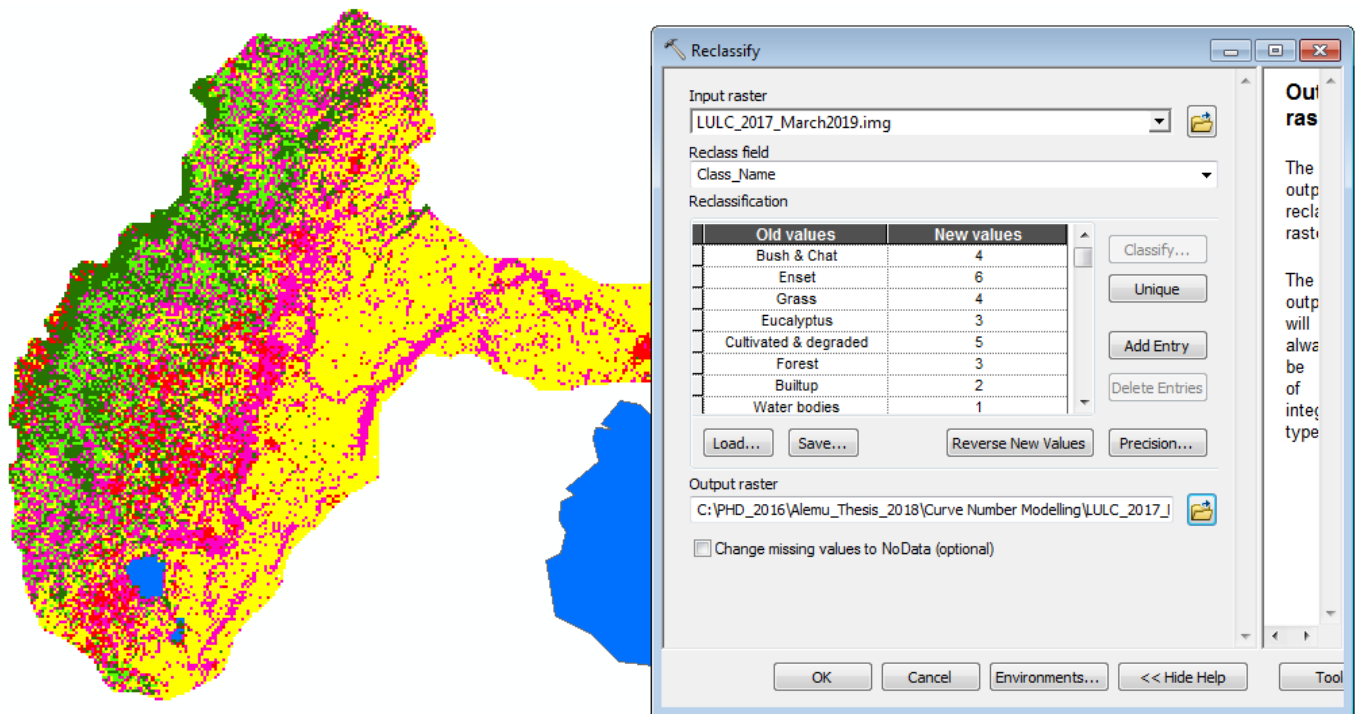


Figure 7: Reclassification window with assigned new values

The final steps in processing land use data were converting the reclassified land use grid (raster) into a polygon feature class following the procedure in Conversion Tools of the Arc Toolbox and assign the new value.

1.1.3. Hydrologic soil groups data preparation for CN grid

The hydrological soil data are collected from Ethiopia Ministry of Water, Irrigation and Energy (MOWE, 2013) as shown in Figure 8 and verified by HWSD viewer. The soil categories such as Cambisol, Andosol, Fluvisol, Leptosol, Vertisol and Luvisol are identified and hydrologic soil group is assigned to each category based on US Natural Resource Conservation Service (NRCS) that may fall into four hydrologic soil groups (HSG) (A, B, C and D): high, moderate, slow and very slow infiltration rates respectively (USDA-NRCS, 1986).

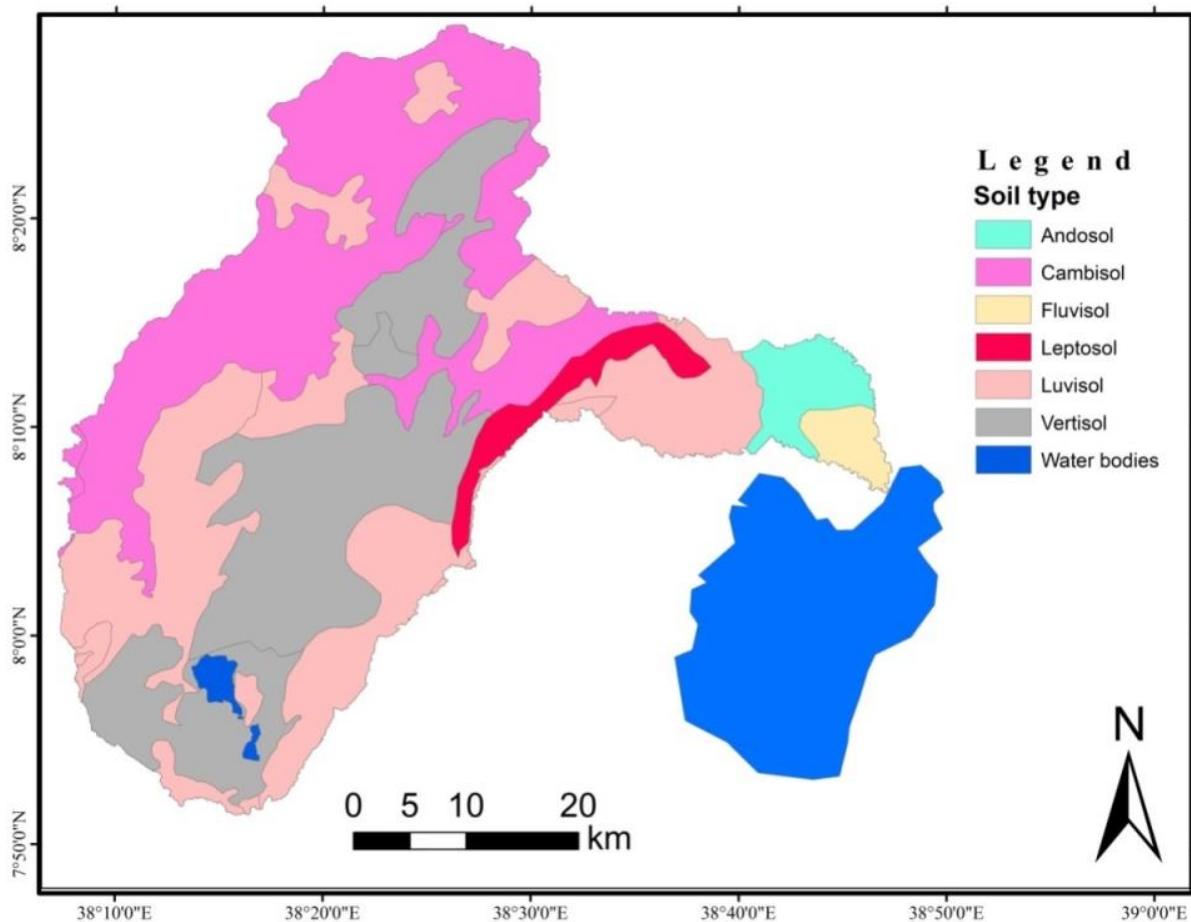


Figure 8: Soil map of the area (MWIE, 2017)

Add Soil_WZ_2018_1 feature class from spatial dataset collected from Ethiopia MOWIE and in its attribute table create an empty field for storing soil group data as shown in Table 5. Hence the hydrologic soil group data can be populated to Soil_WZ_2018_1 after identifying the type of soil with its corresponding description.

Ethiopian Road Authority (2013) manual is used to generate the relationship of soil type and hydrologic soil group of Meki river watershed and also verified by HWSD viewer and also shape file data acquired from MOWIE as shown in Table 5.

Table 5: Hydrologic soil group of different soil types (ERA, 2013)

Soil Types	Hydrologic Soil Group (HSG)	Soil Types	HSG	Soil Types	HSG
Orthic Acrisols	B	Calcaric Fluvisols	B	Eutric Nitosols	B
Chromic Cambisols	B	Eutric Fluvisols	B	Dystric Histosols	D
Dystric Cambisols	B	Chromic Luvisols	B	Eutric Histosols	D
Eutric Cambisols	B	Orthic Luvisols	B	Cambric Arenosols	A
Humic Cambisols	C	Vertic Luvisols	C	Calcaric Regosols	A
Calcic Cambisols	B	Dystric Nitosols	B	Eutric Regosols	A
Vertic Cambisols	B	Calcic Xerosols	B	Humic Andosols	B
Calcic Chernozems	B	Luvic Xerosols	C	Mollic Andosols	B
Rendzinas	D	Gypsic Yermosols	B	Vitric Andosols	B
Haplic Phaeozems	C	Gleyic Solonchaks	D	Chromic Vertisols	D

Luvic Phaeozems	C	Orthic Solonchaks	B	Haplic Xerosols	B
Lithosols	D	Pellic Vertisols	D		

Accordingly, the HSG is assigned to each of the six soil types identified in the watershed as shown in Figure 9. During the assignment the HSG of Leptosol is assigned after referring the field characteristics of the soil and it has more similarity to Luvisol with its insignificant areal coverage to influence the value of the curve number and hence HSG of C is assigned to it.

FID	Shape *	DIGS	DIGSOIL	soil	Area	Area_he	Tex	Soilmappi	Soil	Name	MU_GLO	Soil_WZ_201
6	Polygon	38	0	605	1022	102268.5	1	ANz 2/3 ab	B	Andosol	16903	
1	Polygon	8	0	604	108.	10831.52	3	CMe 3 de	B	Cambisol	16932	
5	Polygon	23	0	7	192.	19203.82	2	CMx 2/3 bc	B	Cambisol	16932	
15	Polygon	10	0	2	635.	63578.44	3	CMe 3 de	B	Cambisol	16964	
14	Polygon	21	0	24	139.	13999.45	1	FLc 1/2 ab	B	Fluvisol	16982	
2	Polygon	9	0	16	69.1	6910.35	3	LP 3 cd	C	Leptosol	16808	
0	Polygon	6	0	607	34.4	3448.9	3	LVh 1/2 cd	C	Luvisol	16739	
3	Polygon	11	0	17	735.	73572.59	2	LVh 1/2 bc	C	Luvisol	16739	
7	Polygon	40	0	6	7.53	752.85	3	LVh 1/2 de	C	Luvisol	16739	
8	Polygon	45	0	10	34.4	3446.04	3	LVh 1/2 de	C	Luvisol	16739	
9	Polygon	3	0	1	17.1	1716.35	2	LVh 1/2 bc	C	Luvisol	16739	
16	Polygon	28	0	11	1570	157018.4	3	LVh 1/2 de	C	Luvisol	16739	
17	Polygon	18	0	15	274.	27427.94	1	LVh 1/2 ab	C	Luvisol	16739	
18	Polygon	50	0	22	180.	18042.89	1	LVh 1/2 ab	C	Luvisol	16739	
19	Polygon	50	0	22	53.9	5391.7	2	LVh 1/2 c	C	Luvisol	16739	
22	Polygon	18	0	15	44.6	4463.49	1	LVh 1/2 ab	C	Luvisol	16739	
23	Polygon	5	0	4	50.2	5028.65	3	LVh 1/2 cd	C	Luvisol	16739	
4	Polygon	18	0	15	342.	34274.01	1	VRe 1 a	D	Vertisol	16851	
10	Polygon	5	0	4	131.	13131.2	2	VRe 1 bc	D	Vertisol	16855	
20	Polygon	50	0	22	683.	68333.52	2	VRe 1 bc	D	Vertisol	16839	
21	Polygon	18	0	15	17.5	1755.23	1	VRe 1 a	D	Vertisol	16851	
11	Polygon	0	0	Wat	2.83	282.53	0		0	Water	16994	
12	Polygon	0	0	Wat	0.1	9.59	0		0	Water	16994	
13	Polygon	0	0	Wat	13.2	1324.4	0		0	Water	16994	

Figure 9: Hydrologic soil group (HSG) assignment

Editing the Soil_WZ_2018_1 and transferring HSG, now we have a Soil Code (soil group) assigned to each polygon in Soil_WZ_2018_1. Following soil group assignment, create four more fields named PctA, PctB, PctC, and PctD all of type short integer in Soil_WZ_2018_1 feature class. For each feature (polygon) in Soil_WZ_2018_1 PctA will define what percentage of area within the polygon has soil group A, PctB will define what percentage of area within the polygon will have soil group B and so on (USDA-NRCS, 1986) . This is critical when we have polygons with more than one soil group (for eg. A-B-A/D would mean that group A, group B and group A/D soils are found in one polygon; A/D would mean the soil behaves as A when drained and as D when not drained, and so on). If we have classifications such as these, we need to define how much area of a polygon is A/B/C/D.

For Meki river watershed area we have only one soil group assigned to each polygon so a polygon with soil group “A” will have PctA = 100, PctB = 0, PctC = 0, and PctD = 0. Similarly for a polygon with soil group D, only PctD = 100, and other three Pcts are 0. Now populate PctA, PctB, PctC and PctD based on Soil Code for each polygon. You can select features based on Soil Code and then use field calculator to assign numbers to polygons. The resulting attribute table should look like as shown in Figure 10.

soil	Area	Area_he	Tex	Soilmappi	Soil	Name	MU_GLO	Soil_WZ_2018_1.HYDROID	Soil_WZ_2018_1.PctA	Soil_WZ_2018_1.PctB	Soil_WZ_2018_1.PctC	Soil_WZ_2018_1.PctD
2	635.	63578.44	3	CMe 3 de	B	Cambisol	16964	16	0	100	0	0
24	139.	13999.45	1	FLc 1/2 ab	B	Fluvisol	16982	15	0	100	0	0
16	69.1	6910.35	3	LP 3 cd	C	Leptosol	16808	3	0	0	100	0
607	34.4	3448.9	3	LVh 1/2 cd	C	Luvisol	16739	1	0	0	100	0
17	735.	73572.59	2	LVh 1/2 bc	C	Luvisol	16739	4	0	0	100	0
6	7.53	752.85	3	LVh 1/2 de	C	Luvisol	16739	8	0	0	100	0
10	34.4	3446.04	3	LVh 1/2 de	C	Luvisol	16739	9	0	0	100	0
1	17.1	1716.35	2	LVh 1/2 bc	C	Luvisol	16739	10	0	0	100	0
11	1570	157018.4	3	LVh 1/2 de	C	Luvisol	16739	17	0	0	100	0
15	274.	27427.94	1	LVh 1/2 ab	C	Luvisol	16739	18	0	0	100	0
22	180.	18042.89	1	LVh 1/2 ab	C	Luvisol	16739	19	0	0	100	0
22	53.9	5391.7	2	LVh 1/2 c	C	Luvisol	16739	20	0	0	100	0
15	44.6	4463.49	1	LVh 1/2 ab	C	Luvisol	16739	23	0	0	100	0
4	50.2	5028.65	3	LVh 1/2 cd	C	Luvisol	16739	24	0	0	100	0
15	342.	34274.01	1	VRe 1 a	D	Vertisol	16851	5	0	0	0	100
4	131.	13131.2	2	VRe 1 bc	D	Vertisol	16855	11	0	0	0	100
22	683.	68333.52	2	VRe 1 bc	D	Vertisol	16839	21	0	0	0	100
15	17.5	1755.23	1	VRe 1 a	D	Vertisol	16851	22	0	0	0	100
Wat	2.83	282.53	0		0	Water	16994	12	0	0	100	0
Wat	0.1	9.59	0		0	Water	16994	13	0	0	100	0
Wat	13.2	1324.4	0		0	Water	16994	14	0	0	100	0

Figure 10: Standard curve number matrix assignment for different soil groups

The preparation of soil data is over at this point. The next step is to merge/union both soil data and land use data to create polygons that have both soil and land use information. Save the map document.

1.1.4. Merging of Soil and Landuse Data

To merge/union soil and land use data, use the Union tool in Arc Tool box available under Analysis Tools - Overlay. Browse/drag Soil_WZ_2018_1 and LULC_2017_March2019Pol as input features, name the output feature class as “Meki_Soil_LU”, leave the default options, and click OK as shown in Figure 11.

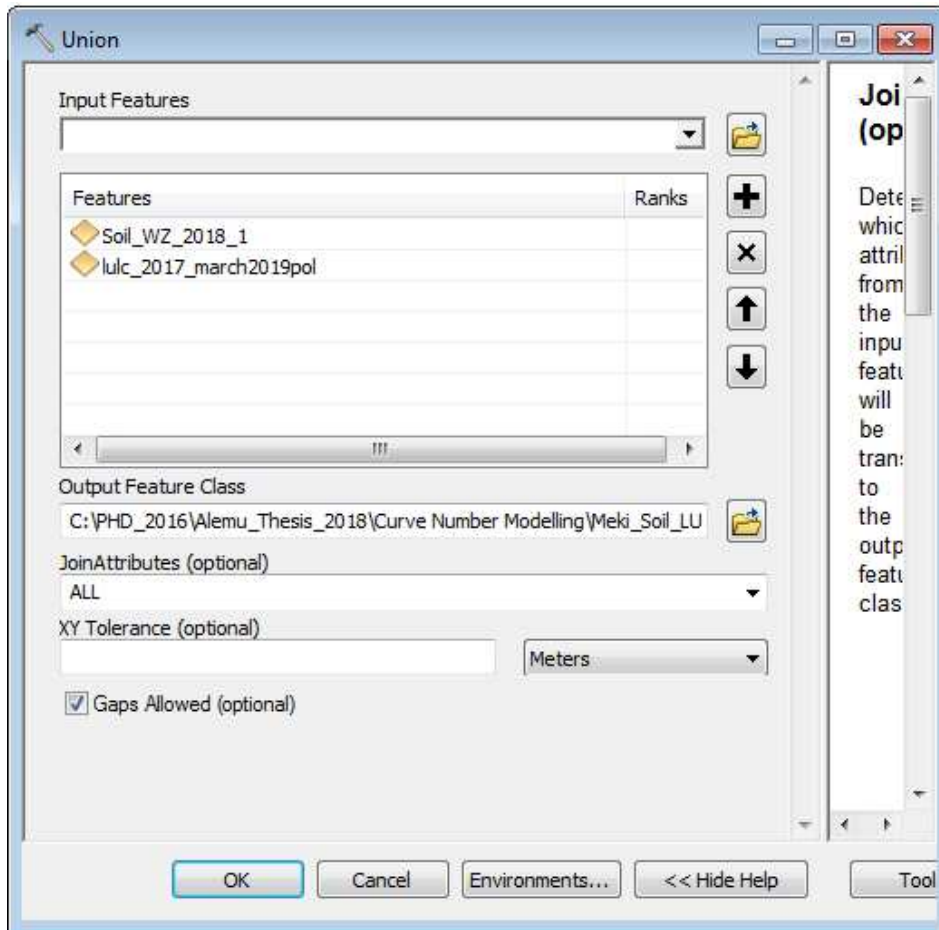


Figure 11: Soil land use union (Merge) of the watershed

The result of union/merge features inherit attributes from both feature classes that are used as input. However, if the outer boundaries of input feature classes do not match exactly, the resulting merged feature class (Meki_Soil_LU in this case) usually will have features that will have attributes from only one feature class called “slivers” because the other feature do not exist in this area.

If we open the attribute table for Meki_Soil_LU, we will find that there are several sliver polygons in this feature class that have attributes only from LULC_2017_March2019Pol and the soil attributes are empty, and vice versa as shown in Figure 12:

FID	Shape	FID_luc	ID	GRID	Valu	FID_Soil_W	DIG	DIGS	soil	Are	Are	Text	Soilm	Name	MU_G	HSG	HYDROID	PctA	PctB	PctC	PctD
0	Polygon	0	1	5	5	-1	0	0		0	0	0			0		0	0	0	0	0
1	Polygon	1	2	4	4	-1	0	0		0	0	0			0		0	0	0	0	0
2	Polygon	2	3	6	6	-1	0	0		0	0	0			0		0	0	0	0	0
3	Polygon	4	5	3	3	-1	0	0		0	0	0			0		0	0	0	0	0
4	Polygon	6	7	5	5	-1	0	0		0	0	0			0		0	0	0	0	0
5	Polygon	7	8	4	4	-1	0	0		0	0	0			0		0	0	0	0	0
6	Polygon	10	11	5	5	-1	0	0		0	0	0			0		0	0	0	0	0
7	Polygon	11	12	4	4	-1	0	0		0	0	0			0		0	0	0	0	0
8	Polygon	14	15	3	3	-1	0	0		0	0	0			0		0	0	0	0	0
9	Polygon	15	16	4	4	-1	0	0		0	0	0			0		0	0	0	0	0
1	Polygon	16	17	5	5	-1	0	0		0	0	0			0		0	0	0	0	0
1	Polygon	19	20	3	3	-1	0	0		0	0	0			0		0	0	0	0	0
1	Polygon	22	23	6	6	-1	0	0		0	0	0			0		0	0	0	0	0
1	Polygon	23	24	4	4	-1	0	0		0	0	0			0		0	0	0	0	0
1	Polygon	24	25	5	5	-1	0	0		0	0	0			0		0	0	0	0	0
1	Polygon	25	26	4	4	-1	0	0		0	0	0			0		0	0	0	0	0
1	Polygon	32	33	6	6	-1	0	0		0	0	0			0		0	0	0	0	0
1	Polygon	33	34	5	5	-1	0	0		0	0	0			0		0	0	0	0	0
1	Polygon	46	47	6	6	-1	0	0		0	0	0			0		0	0	0	0	0
1	Polygon	47	48	4	4	-1	0	0		0	0	0			0		0	0	0	0	0
2	Polygon	48	49	3	3	-1	0	0		0	0	0			0		0	0	0	0	0
2	Polygon	49	50	5	5	-1	0	0		0	0	0			0		0	0	0	0	0

Figure 12: Avoiding sliver (-1) of the soil land use union of the watershed

One way to deal with sliver polygons is to assign missing values to all features or (easiest!) is to just delete them (Merwade, 2012).

1.1.5. Creating CN Look-up table

The next step is to prepare a look-up table that will have curve numbers for different combinations of land uses and soil groups. In this case, we will use SCS curve numbers that are available from the literature. The spatial features in conjunction with the lookup table can then be used to create curve number grid (Merwade, 2012).

Create a table named "CNLookUp". In Arc tool box, select Data Management Tools ... Table ... Create Table. Now start the Editor to edit the newly created CNLookUp table, and populate it as shown in Figure 13.

Rowid	OBJEC	FIEL	LUVALUE	DESCRIPTION	A	B	C	D
1	0	0	1	Water bodies	100	100	100	100
3	0	0	2	Builtup	77	85	90	92
5	0	0	3	Eucalyptus/Forest	36	60	73	79
7	0	0	4	Bush & Chat/Grass	49	69	79	84
9	0	0	5	Cultivated & degraded	67	78	85	89
11	0	0	6	Enset	39	52	58	62

Figure 13: Lookup table considering EBLUS

Columns A/B/C/D store curve numbers for corresponding soil groups for each land use system (LUValue) that are obtained from Ethiopian Road Authority (2013), USDA-NRCS (1986) and the model output for EBLUS.

1.1.6. Creating CN Grid

HEC-GeoHMS uses the merged feature class (Meki_Soil_LU) and the lookup table (CNLookUp) to create the curve number grid. A field created in the merged feature class (Meki_Soil_LU) named "LandUse" that will have land use category information to link it to CNLookUp table. We already have this information stored in GRIDCODE field, but HEC-GeoHMS looks for this information in LandUse field. So create a field named LandUse (type: short integer), and populate it by equating it to GRIDCODE.

On the HEC-GeoHMS Project View toolbar, click on Utility ... Create Parameter Grids... Choose the lookup parameter as Curve Number (which is the default), Click OK, and then select the inputs as shown in Figure 14.

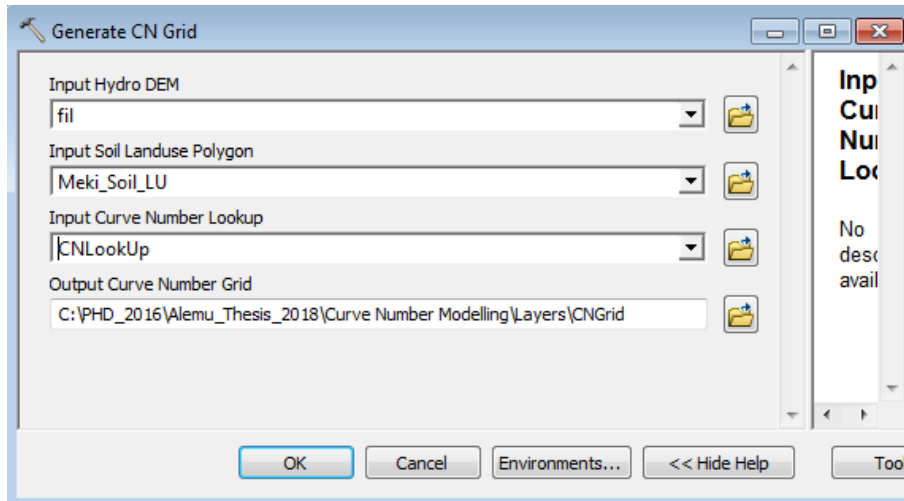


Figure 14: CN generation considering Enset-Based land use system

Fil for Hydro DEM, Meki_Soil_LU (merged soil and land use) for input soil landuse polygon, CNLookUp table for input Curve Number Lookup, and leave the default CNGrid name for the Curve Number Grid.

2.8. Determination of watershed based curve number

Curve number is extracted from the soil type and land use data considering EBLUS using HEC-GeoHMS, which both affect the infiltration capacity of the soil and the Soil data acquired from the Ethiopian Ministry of Water Irrigation and Energy (MWIE) and Landsat image from USGS (Fleming and Brauer, 2018).

The factors of the CN model developed from the raster format of soil and LUS data with the same coordinate system (UTM WGS 1984 37⁰ North) with a spatial resolution of 30m. Finally, the result is extracted and reported for the classified LUS of Meki river watershed and also it is extracted to 34 sub-watersheds and two major growing zones (Enset growing and non-Enset growing zones) of Meki river watershed.

3. Result and Discussion

3.1. Infiltration capacity of the soil

Field data were collected, summarized and presented in **Error! Reference source not found.** of appendix for the infiltration capacity of the soil for different land use systems. The silt loam and clay loam textural classes are dominant in the upper zone while almost all textural classes are found in the middle zone of the watershed. According to Oliver *et al* 2006, the soil textural class of Meki river watershed is dominantly occupied by Sandy Loam, Silt Loam, Clay Loam and Clay irrespective of the land use systems with a range of infiltration rate values of 20 to 30mm/hr, 10 to 20mm/hr, 5 to 10mm/hr and 0 to 5mm/hr respectively. EBLUS is not commonly practiced in acacia wooded grass land of Rift valley for which measurement is not done. Hence, the infiltration rate of soils in the acacia wooded grass land is not measured because of our focus was comparison of land use systems which are found in the same zone and the same soil type with EBLUS and the average value is presented in Table 6.

Sandy loam soil textural class has higher infiltration capacity than other textural classes followed by silt loam in all land use systems. High infiltration capacity is measured in the natural forest covered portion of the watershed followed by EBLUS. EBLUS improves the infiltration and water holding capacity of the soil by increasing the organic matter content of the soil through litter and pseudo stem cover falls and also the root fiber of 2 to 3 meters long away from the edge of the pseudo stem measured in the field that can enhance the void space of the soil to transmit rain water easily to the ground. The presence of wide leaves protects the direct impact

of the rain drop (Kebede Wolka, et al, 2015) and permit more through fall which reduces the speed of the rain drop and it will give more time for rain water to infiltrate to the ground.

Table 6: Mean infiltration rate of land uses

Land Use	Soil Texture	Mean Infiltration Rate (mm/Hour)		Maen infiltration rate for LUSs	Basic infiltration rate (mm/hour) (Oliver, Niels, Hogler, & Reinhard, 2006)
		Upper zone	Middle zone		
Cultivated LUS	Sandy Loam		19.125	10.375	20 to 30
	Silt Loam	12	13.9625		10 to 20
	Clay Loam	7.2125	5.825		5 to 10
	Clay		4.125		1 to 5
Built up & degraded LUS	Sandy Loam		8.75	7.0625	20 to 30
	Silt Loam	7.0625	10		10 to 20
	Clay Loam		5.5		5 to 10
	Clay		4		1 to 5
Grass land & planted forest LUS	Sandy Loam		19.25	11.1875	20 to 30
	Silt Loam	15.8625	9.95		10 to 20
	Clay Loam	8.6	7.9625		5 to 10
	Clay		5.5		1 to 5
EBLUS	Sandy Loam		22.55	12.8125	20 to 30
	Silt Loam	12.625	17.025		10 to 20
	Clay Loam	10.875	9.375		5 to 10
	Clay		4.425		1 to 5
Natural Forest LUS	Sandy Loam		22.625	12.9675	20 to 30
	Silt Loam	15.25	15.5		10 to 20
	Clay Loam	9.625	10.3475		5 to 10
	Clay		4.4575		1 to 5
Average		11.0125	10.92625		

The Upper zone of the watershed has higher mean infiltration rate (11.0125mm/hr) than the Middle zone (10.92625mm/hr) of the watershed. The high mean infiltration rate at the upper zone shows the presence of more forest LUS and EBLUS than the middle zone of the watershed which enhances infiltration and water holding capacity of the soil. In the cultivated LUS, high

rate of infiltration is recorded in upper zone of the watershed while middle zone has more infiltration rates in Grass LUS, forest LUS and EBLUS as shown in Figure 15, which is attributed to the high slope of upper zone that influences the carbon stock of the soil.

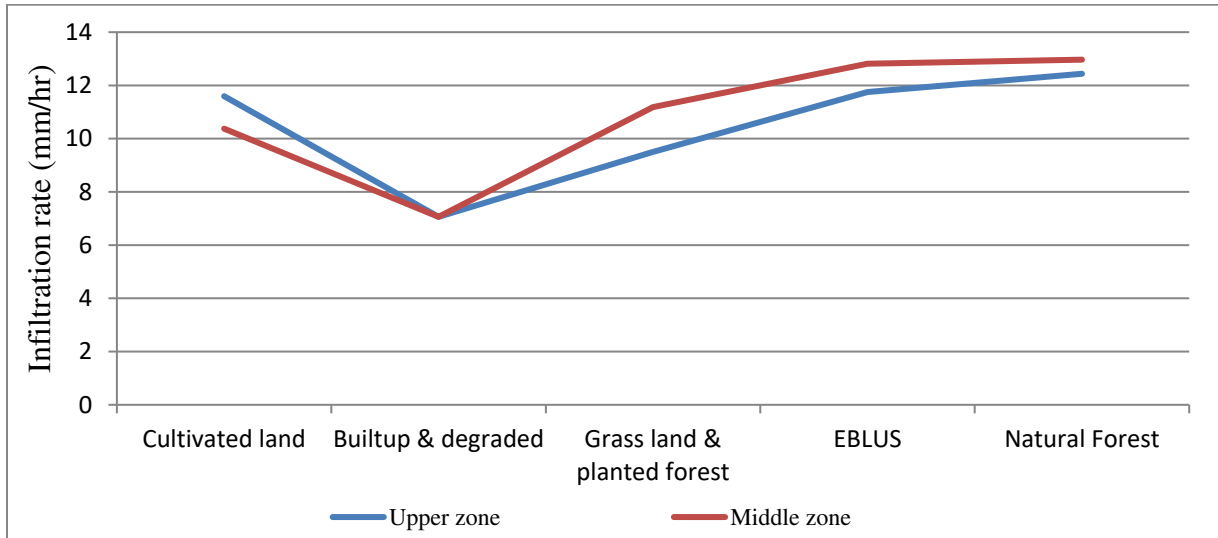


Figure 15: Vegetation zone based infiltration capacity of the soil (mm/hr)

There is a significant difference between infiltration rates at different land use systems at 5% significance level ($\alpha = 0.05$) with a p-value of 0.0094 ($<\alpha$) due to a low value in the Built-up & degraded and cultivated LUS and a high value in Forests and EBLUS and a non-significance difference is observed between infiltration rates among vegetation zones with p-value of 0.443 ($>\alpha$) as shown in Table 7.

Table 7: Analysis of variance (ANOVA)

Source of Variation	SS	df	MS	F	P-value	F crit
Land use systems	40.16427	4	10.04107	16.51739	0.009404	6.388233
Vegetation zone	0.440475	1	0.440475	0.724574	0.442606	7.708647
Error	2.431635	4	0.607909			
Total	43.03638	9				

Therefore, a high mean infiltration rate in Forests and EBLUS show that there is an improvement in hydrological parameters for those land use systems to enhance water absorption to the ground water system. The improvement in infiltration capacity has a direct influence on water resources management. In addition, the increase in infiltration rate has a huge contribution in runoff reduction and alleviation of sedimentation problems in Meki river watershed.

3.2. Curve number modeling result

Soil Conservation Curve Number (SCS-CN) is an empirically derived relationship between location, land use, antecedent moisture conditions and runoff and it is used in many event-based models to establish the initial soil moisture condition and the infiltration characteristics (Iliasse & Adil, 2014). There is an inverse relationship between infiltration capacity and the runoff generation capacity of the area (A.R., H.A., & S.H.R., 2010; Zehetner & Miller, 2006; Zeiger & Fohrer, 2009); hence the infiltration capacity of the soil is considered as one of the criteria to model the curve number of EBLUS.

Studies showed that organic matter influences CN and results in low surface runoff due to an increasing in soil infiltration capacity (A.R., H.A., & S.H.R., 2010; Zehetner & Miller, 2006; Zeiger & Fohrer, 2009). According to Mesfin, et al (2017) and Barbora and Jaroslava (2014), compost improves and accelerated both the infiltration and water holding capacity of the soil for a longer period which in turn influences the CN of the watershed.

EBLUS exhibited a good carbon sequestration, which is equivalent to high-vegetation areas (Mesfin et al., 2017). Hence, Carbon stock considered as criteria to model the curve number of EBLUS next to the infiltration capacity of the soil as reported in Table 8.

Table 8: Hydrologic Soil Group based curve number of different LULCs excluding Enset LULC (Iliasse and Adil, 2014; ERA, 2013)

Land Cover/Land Use	Hydrologic Soil Group				Parameters to develop the CN model	
	A	B	C	D	Carbon stock (ton/yr)	Average Infiltration (mm/hr)
Open Water	100	100	100	100	0	0
Built-up, Medium Intensity LUS	77	85	90	92	132	7.0625
Natural Forest LUS	36	60	73	79	45,714	12.9675
Grasslands & plantations LUS	49	69	79	84	8350	11.1875
Cultivated LUS	67	78	85	89	19,950	10.375
EBLUS					77,286	12.8125

Therefore, considering the infiltration capacity of forest LUS, grass LUS, cultivated LUS and built-up LUS and their Carbon stock, the following formulas are derived to compute the curve number matrix of EBLUS relative to the other land use systems dominantly practiced in the study area.

$$EA = \frac{\sum_{i=1}^n EAi}{n} = \frac{Ci(FA*IF+GA*IG+CA*IC+BA*IB)}{IE} + \frac{CSq(FA*SqF+GA*SqG+CA*SqC+BA*SqB)}{SqE} \quad \text{Eqn1}$$

$$EB = \frac{\sum_{i=1}^n EBi}{n} = \frac{Ci(FB*IF+GB*IG+CB*IC+BB*IB)}{IE} + \frac{CSq(FB*SqF+GB*SqG+CB*SqC+BB*SqB)}{SqE} \quad \text{Eqn2}$$

$$EC = \frac{\sum_{i=1}^n ECi}{n} = \frac{Ci(FC*IF+GC*IG+CC*IC+BC*IB)}{IE} + \frac{CSq(FC*SqF+GC*SqG+CC*SqC+BC*SqB)}{SqE} \quad \text{Eqn3}$$

$$ED = \frac{\sum_{i=1}^n EDi}{n} = \frac{Ci(FD*IF+GD*IG+CD*IC+BD*IB)}{IE} + \frac{CSq(FD*SqF+GD*SqG+CD*SqC+BD*SqB)}{SqE} \quad \text{Eqn4}$$

Where;

EA, EB, EC and ED are CN of EBLUS for HSG of A, B, C and D respectively

FA, FB, FC and FD are CN of Forest LUS for HSG of A, B, C and D respectively

GA, GB, GC and GD are CN of Grass LUS for HSG of A, B, C and D respectively

CA, CB, CC and CD are CN of Cultivated LUS for HSG of A, B, C and D respectively

BA, BB, BC and BD are CN of Built-up LUS for HSG of A, B, C and D respectively

IE, IF, IG, IC and IB are infiltration capacity of EBLUS, Forest, Grass, Cultivated and Built-up LUSs respectively.

SqE, SqF, SqG, SqC and SqB are Carbon stock of EBLUS, Forest, Grass, Cultivated and Built-up land use systems respectively.

Ci and CSq are coefficients for the relative influence of infiltration capacity and Carbon stock on curve number of land use systems respectively at 85% to 15% proportion.

Accordingly, the curve numbers are generated for EBLUS for each hydrologic soil group with their respective infiltration capacity and Carbon stock relative to other LUSs for which curve number is encoded and presented in Table 9. Carbon stock is modified by growth period and energy production of those LUSs. Hence, infiltration capacity of the soil powers 85% of the curve number of LUSs while 15% of the curve numbers of LUSs are influenced by carbon stock which is computed.

Table 9: Curve number of EBLUS

Curve number	Hydrologic Soil Group (HSG)			
	A	B	C	D
CN of EBLUS due to Infiltration capacity				
$EI1 = \frac{BA * IB}{IE}$	42.44	46.854	49.61	50.712
$EI2 = \frac{FA * IF}{IE}$	36.44	60.73	73.88	79.96
$EI3 = \frac{GA * IG}{IE}$	42.79	60.25	68.98	73.35
$EI4 = \frac{CA * IC}{IE}$	54.25	63.16	68.83	72.068

CN of EBLUS due to Carbon stock	A	B	C	D
$ESq1 = \frac{BA * SqB}{SqE}$	0.13	0.145	0.154	0.16
$ESq2 = \frac{FA * SqF}{SqE}$	21.294	35.49	43.18	46.73
$ESq3 = \frac{GA * SqG}{SqE}$	5.294	7.455	8.54	9.075
$ESq4 = \frac{CA * SqC}{SqE}$	17.295	20.13	21.94	22.97
Cumulative CN of EBLUS for different HSG	A	B	C	D
$E = \frac{0.85 * \sum_{i=1}^4 Eli + 0.15 * \sum_{i=1}^4 ESqi}{4}$	39	51.5	58.3	61.6

Therefore, finally the general formula developed for EBLUS is given as:

$$E = \frac{0.85 * \sum_{i=1}^n Eli + 0.15 * \sum_{i=1}^n ESqi}{n} \quad \text{Alemu's formula}$$

Where:

Eli = Infiltration based Curve number of EBLUS relative to i LUS

ESqi = Carbon stock based Curve number of EBLUS relative to i LUS

Curve number matrix is computed for EBLUS using the model as 39, 51.5, 58.3 and 61.6 for HSG of A, B, C and D respectively. Therefore, the new lookup table for all land use systems including EBLUS is prepared as shown in Table 10 and fed to HEC-GEO-HMS together with that of the union of LUS and soil information in order to generate the curve number grid.

Table 10: Hydrologic Soil Group based curve number of different LUSs including EBLUS

Land Cover/Land Use	Hydrologic Soil Group			
	A	B	C	D
Open Water	100	100	100	100
Builtup, Medium Intensity	77	85	90	92
Natural Forest	36	60	73	79
Grasslands (Pasture) & plantation lands	49	69	79	84
Cultivated land	67	78	85	89

EBLULC	39	51.5	58.3	61.6
---------------	-----------	-------------	-------------	-------------

Hence, the new CN matrix of the Meki river watershed is generated from the new lookup table including EBLUS and mapped as shown in Figure 16. This CN grid can be used in different models of rainfall-runoff modeling purposes and also researchers and runoff flow simulators.

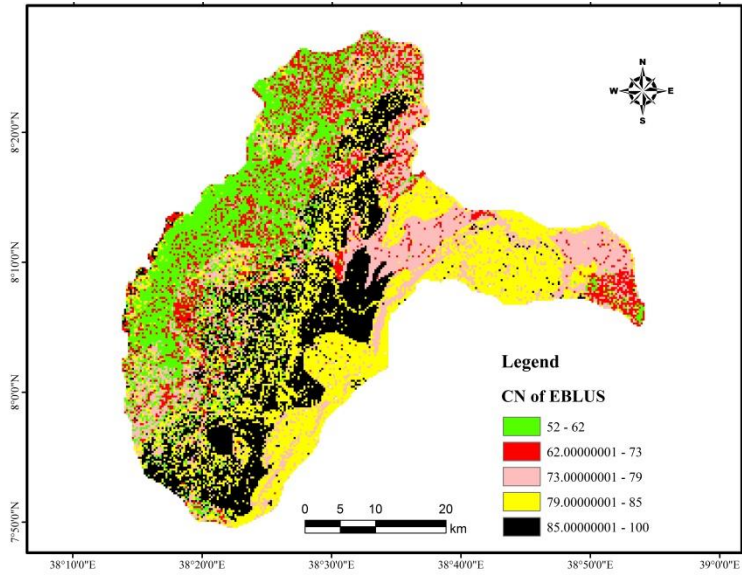


Figure 16: Average soil loss from sub-watersheds with respect to Rift valley limit

3.3. Zone and sub-watershed based CN determination

CN of EBLUS is evaluated for two enset growing zones of Meki river watershed and the mean values of the upper zone is less than the middle one due to the high proportion of forest and EBLUS in the upper zone of the watershed as shown in Table 11.

Table 11: CN of zones of Meki river watershed

Zones	Upper	Middle
Minimum	52	52

Mean	72.78	83.27
Maximum	100	92

Almost all upper zone Sub-watersheds except U9 have a mean CN value of less than 80 while almost all middle zone Sub-watersheds have a mean CN of more than 80 except M1 and M3 as shown in Figure 17.

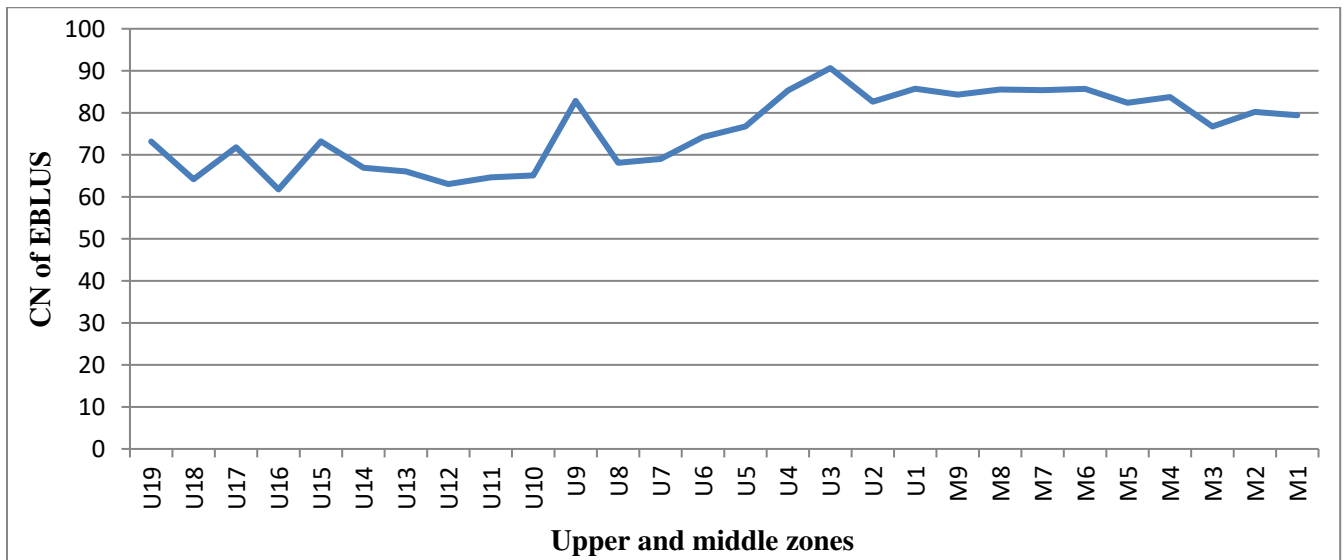


Figure 17: Curve number of EBLUS in the upper and middle zones

3.4. Scenarios on mean CN of Meki river watershed with respect to EBLUS

Meki river watershed has a mean CN of 78.21 considering EBLUS as it has its own CN matrix while a mean CN of 81.72 by considering EBLUS as cultivated LUS as shown in the Table 12 below.

Table 12: Area coverage and average CN of land uses

LU	Area (km ²)	Mean CN, EBLUS as	Mean CN, EBLUS as a	Area (%)
----	-------------------------	-------------------	---------------------	----------

		separate LUS	cultivated LUS	
EBLUS	247.59	56.15	77.26	10.65
Cultivated LUS	964.05	77.26	77.26	41.46
Bush and Chat LUS	595.59	76.87	76.87	25.61
Forest and plantation LUS	328.98	69.1	69.06	14.15
Urban (Built up) LUS	171.69	89.86	89.86	7.38
Water bodies	17.4	100	100	0.75

The mean CN of Meki river watershed considering and without considering EBLUS are 78.21 and 81.72 respectively, hence, the sorptivity and initial abstraction of the watershed decreases as CN increases as shown in Table 13.

Table 13: Initial abstraction and soil retention in millimeters

	CN	Sorptivity = $S = \frac{25400}{CN} - 254$	Initial abstraction (Ia) = 0.2S	0.8S
With	78.2066			
	7	70.7804961	14.1560992	56.6243969
WO	81.7181			
	3	56.8245439	11.3649088	45.4596351

The CN of EBLUS is computed with respect to other LUSs. According to Chow et al, (1988) and Merwade (2012), the precipitation excess is a function of cumulative precipitation, soil type, land use systems and antecedent moisture. Considering the initial loss and the potential maximum retention, the precipitation excess can be calculated; the maximum retention and the basin characteristics are related through the curve number. The standard SCS curve number method is based on the following relationship between rainfall depth, P, and runoff depth, Q

(USDA, 1986; Schulze et al., 1992) which can easily be simulated using HEC-HMS using the CN as an input.

For the annual daily average rainfall of 50mm for Meki river watershed (ENMA, 2017), the runoff considering and without considering EBLUS is computed respectively as:

$$Q_1 = \frac{(P-0.2S_1)^2}{(P+0.8S_1)} = \frac{(50-14.156)^2}{(50+56.6244)} = \frac{1284.792336}{106.6244} = 12.05\text{mm and} \quad (\text{Chow et al, 1988})$$

$$Q_2 = \frac{(P-0.2S_2)^2}{(P+0.8S_2)} = \frac{(50-11.365)^2}{(50+45.46)} = \frac{1492.663225}{95.46} = 15.6366 \text{ mm}$$

Where: Q is surface runoff (mm), P is precipitation (mm), S is the soil retention (Sorpitivity) (mm) and Ia is initial abstraction or initial loss (mm) and CN is curve number

Hence a difference of runoff occurs due to consideration of EBLUS by 3.59 mm which can be cumulate to a huge volume of runoff (8340916m³) from the whole area of Meki river watershed which can be a sign post for the improvement of the hydrological characteristics of the watershed by increasing the infiltration capacity of the soil.

Conclusion& Recommendation

Conclusion

Meki river watershed is dominantly covered by cultivated LUS (41.5%) followed by Bush and Chat LUSs (25.6%). EBLUS comprises about 10.65% of the watershed while Forest and plantations LUSs cover (14.14%) while urban and built up LUSs covers 7.4% with minimal portion is covered by water bodies including wetland (0.75%). Uppermost part of the Meki river watershed is covered by Erica, Enset and natural forest land use systems, while the middle and lower altitudes of the watershed is dominantly covered by agricultural LUSs.

The CN grid in a Meki river watershed can be used as an input for different research purposes concerning direct runoff generation capacity of the area. There is an improvement of average CN from 81.72 to 78.21 for the whole watershed. A significant volume of water (8340916m³) is infiltrated due to the presence of EBLUS in the watershed.

Therefore, a high mean infiltration rate in Forests and EBLUS shows that there is an improvement in hydrological parameters for those LUSs to enhance water absorption into the ground water system. The improvement in infiltration capacity has a direct influence on water resources management. In addition, the increase in infiltration rate has a huge contribution in runoff reduction and alleviation of sedimentation problems in the Meki river watershed.

Recommendation

A significant CN reduction due to EBLUS shows there will be an improvement in the hydrological characteristics of the watershed by increasing the infiltration capacity of the soil and also by increasing the canopy cover of the area. Hence, increasing the coverage of EBLUS can reduce the CN and runoff volume which could be the cause of flooding in different parts of the watershed and also protect Lake Ziway against sedimentation.

Therefore, creating separate land use policy to EBLUS and incorporating other fruit as an agro-forestry to it will create harmony to the existing ecology. The extension program has to be initiated to the expansive production and processing of EBLUS which can help the production of sufficient inputs to the industries to be established in the area.

Abbreviations

DEM	Digital Elevation Model
EBLUS	Enset-Based Land Use System
EGSIA	Ethiopian geospatial information agency
ENMA	Ethiopian National Meteorological Agency

ERA	Ethiopian Road Authority
ERDAS	Earth Resources Data Acquisition System
GIS	Geographical Information System
GPS	Geographical Positioning System
HEC-GEO-HMS	Hydrologic Engineering Center's Geospatial Hydrologic Modeling System
HEC-HMS	Hydrologic Engineering Center's Hydrologic Modeling System
HSG	Hydrologic Soil Group
HWSD	Harmonized World Soil Data
LULCC	Land Uses and Land Cover Change
LUSs	Land use systems
m.a.s.l.	Meter above Sea Level
MOWIE	Ministry of Water, Irrigation and Energy
SCS-CN	Soil Conservation Services Curve Number

DECLARATION

Originality of work

We assure that, this paper is the original work and have not been presented for a degree in any other university, and all sources of material used for this paper have been duly acknowledged.

Ethics approval and consent to participate

'Not applicable'

Consent for publication

'Not applicable'

Availability of data and material

Data are acquired from Ministry of Water, Irrigation & Electricity (MOWIE) of Ethiopia for flow data, Ethiopian Meteorological Agency (EMA) for meteorological data, Ethiopian Central Statistical Agency (ECSA) for population data, Ethiopian Geospatial & Mapping Agency (EGMA) for Satellite images and topo-maps, Satellite images from USGS earth explorer and field materials acquired from Ethiopian Institute of Water Resources (EIWR) in Addis Ababa University.

Competing interests

"The authors declare that they have no competing interests"

Funding

Our research is funded by Addis Ababa University (Student grant and thematic research fund)

Authors' contributions

Authors in this article made substantial contributions to the conception and design of the work; the acquisition, analysis and interpretation of data and finally have drafted the work or substantively revised it together and the authors read and approved the final manuscript.

Acknowledgements

Thanks to God for being with us. We gratefully acknowledge the contributions of Dr Feleke Zewge and Dr. Bikila from Addis Ababa University, College of Natural and Computational

Sciences and Mr Mamo Kassegn from Ethiopian institute of water resources. We want to express our greatest appreciation to Ministry of Water, Irrigation and Electricity (MOWIE) of Ethiopia and National Meteorological Agencies (NMA), Ethiopian Central Statistical Agency (ECSA), Ethiopian Geospatial & Mapping Agency (EGMA) and Ethiopian Institute of Water Resources (EIWR) of Addis Ababa University for providing necessary data, materials, equipment and information for this study.

This research was also supported in part by thematic research fund of Addis Ababa University, College of Natural and Computational Sciences, Department of Biology and also supported by student fund from Ethiopian Institute of Water Resources (EIWR) in Addis Ababa University.

Reference

- A. R. , V., H. A. , B., & S. H. R. , S. (2010). Modeling relationship between runoff and soil properties in dry-farming lands, NW Iran. *Hydrology and Earth System Sciences (HESS)*, 7, 2577–2607.
- A., P. N., B., J. W., & J., D. M. (2011). Evaluating the impacts of land use changes on hydrologic responses in the agricultural regions of Michigan and Wisconsin.
- A.O.Ibeje, J. a. (2018). Impact of land use on infiltration. *World journal of Engineering Research and Technology*, 4 (6), 95 -102.
- Admasu Tsegaye 1 and P.C.Struik2 (2003). Growth, radiation use efficiency and yield potential of enset (*Ensete ventricosum*) at different sites in southern Ethiopia. *Ann. appl. Biol.*, 142, 71-81.
- Admasu, T. (2007). Effect of repetitive transplanting & leaf pruning on growth and dry matter partitioning of Enset. *Agronomy*, 6(1), 45-52.
- Alemu Beyene, Sebsebe Demisew, Mekuria Argaw, Azage Gebreyohannes (2020). Enset-Based land use land cover change detection and its impact on soil erosion in Meki river watershed, Western Lake Ziway Sub-Basin, Central Rift Valley of Ethiopia, *International Journal of Environmental Systems Research / Journal code: 40068-020-00198-x _Article- Ms Code: ENSR-D-20-00048*.
- Anita S., Haile B., Tesfaye S., Abebe Y., Amaldegn A. and Tabogie E. (1996). Enset Farming Systems in Southern Region, Ethiopia. Report on a Rapid Rural Appraisal in Gurage,

- Hadiya and Sidama Zones, University of Florida. Deutsche Gesellschaft for Technische Zusammenarbeit (GTZ), 83.
- Barbora, B., & Jaroslava, B. (2014). Effect of various compost doses on the soil infiltration capacity. 62.
- BRIDGE, W. P. (1992). The lesion nematode *pratylenchus goodeyi*, an important pest of Ensete in Ethiopia. *Tropical pest management*, 38(3), 325-326.
- Burch, G., Bath, R., Moore, I., & O'Loughlin, E. (1987). A comparative hydrological behavior of forested and cleared catchments in south eastern Australia. *Journal of Hydrology*, 90, 19-42.
- Chow, V. T., R.Maidment, D., & Mays, L. W. (1988). *APPLIED HYDROLOGY*. New York St. Louis San Francisco Auckland Bogota Caracas Lisbon London Madrid Mexico City Milan Montreal New Delhi San Juan Singapore Sydney Tokyo Toronto: McGraw-Hill, Inc.
- Ethiopia Minister of Water and Energy (2013). Strategic agenda for adaptation to urban water-mediated impacts of climate change in Addis Ababa, Federal Democratic Republic of Ethiopia.
- Iliasse Khaddor and AdilHafidiAlaoui (2014). Production of a Curve Number map for Hydrological simulation - Case study: Kalaya Watershed located in Northern Morocco. *International Journal of Innovation and Applied Studies*. ISSN 2028-9324 Vol. 9 No. 4 Dec. 2014, pp. 1691-1699 © 2014 Innovative Space of Scientific Research Journals <http://www.ijias.issr-journals.org/>
- Elfert , S., & Bormann, H. (2010). Simulated impact of past and possible future land use changes on the hydrological response of the Northern German lowland 'Hunte' catchment. *J HYDROL*, 383, 245– 255.

- Elias, A. A. (2011). Soil Nutrient Evaluation under Different Land Use Types in the Smallholder Farming Systems of Jimma Zone, Ethiopia. *International Journal of Agricultural Research*, 6(9), 707-713.
- ENMA (2017). Ethiopian National Meteorological Agency data analysis, Addis Ababa, Ethiopia
Ethiopian Road Authority (ERA) (2013). Drainage Design Manual, Addis Ababa, Ethiopia.
- Feddema, J., Oleson, K., Bonan, G., Mearns, L., Buja, L., Meehl, G., et al. (2005). The importance of land-cover change in simulating future climates. *SCIENCE*, 310(5754), 1674-1678.
- Ghaffari, G., Keesstra, S., Ghodousi, J., & Ahmadi, H. (2010). SWAT-simulated hydrological impact of land-use change in the Zanjanrood Basin, Northwest Iran. *HYDROL PROCESS*, 24(7), 892-903.
- James Harrison 1, K. A. (2014). A Draft Genome Sequence for *Ensete ventricosum*, the Drought-Tolerant “Tree Against Hunger”. *Agronomy*, 4, 13-33.
- Jerzy , R., Anna , R.-P., & Jan , R. (2014). The Effect of Land Use Change on Transformation of Relief and Modification of Soils in Undulating Loess Area of East Poland. *Scientific World Journal*, 2014(341804).
- Kebede Wolka, Habitamu Tadesse, Efreem Garedew and Fantaw Yimer (2015). Soil erosion risk assessment in the Chaleleka wetland watershed, Central Rift Valley of Ethiopia, *Environmental Systems Research* (2015) 4:5, DOI 10.1186/s40068-015-0030-5.
- M. Fleming and T. Brauer (2018). Hydrologic Modeling System HEC-HMS Quick Start Guide, US Army Corps of Engineers, Institute of Water Resources, Hydrologic Engineering Center, 609 Second Street, Davis CA 95616-4687.

- Mbow, C., Van Noordwijk, M., Luedeling, E., Neufeldt, H., Minang, A., & Kowero, G. (2014). Agroforestry solutions to address food security and climate change challenges in Africa. *Curr. Opin. Environ. Sustain.* 6:61–67. <https://doi.org/10.1016/>.
- Merwade, V. (2012). Creating SCS Curve Number Grid using HEC-GeoHMS. School of Civil Engineering, Purdue University. vmerwade@purdue.edu, 1-26.
- Mesfin, S., Christine, F., & Kumlachew, Y. (2018). Plant diversity analysis for conservation of Afromontane vegetation in socio-ecological mountain landscape of Gurage, South Central Ethiopia. *International Journal of Biodiversity and Conservation*, 10(4), 161-171.
- Mesfin, S., Osamu, S., Christine, F., & Kumelachew, Y. (2017). Quantification and mapping of the supply of and demand for carbon storage and sequestration service in woody biomass and soil to mitigate climate change in the socio-ecological environment table 5 of pp 349.
- MOWE (2013). Strategic agenda for adaptation to urban water-mediated impacts of climate change in Addis Ababa, Federal Democratic Republic of Ethiopia. Addis Ababa.
- Nyssen, J., Habtamu, T., Mulugeta, L., Amanuel, Z., Nigussie, H., & Mitiku, H. (2008). Spatial and temporal variation of soil organic carbon stocks in a lake retreat area of the Ethiopian Rift Valley. *Geoderma*, 146, 261–268.
- Okirya Martin, Albert Rugumayo and Janka Ovcharovichova (2012). Application of Hec-Hms/Ras and GIS Tools in Flood Modeling: A Case Study for River Sironko, UGANDA. *GLOBAL Journal of engineering, design & technology*.

- Oliver B., Niels A. W., Hogler F., and Reinhard F. H. (2006). Water infiltration and hydraulic conductivity in sandy cambisols: impacts of forest transformation on soil hydrological properties.
- Oliver, B., Niels, A. W., Hogler, F., & Reinhard, F. H. (2006). Water infiltration and hydraulic conductivity in sandy cambisols: impacts of forest transformation on soil hydrological properties.
- Qiu, Y., Jia, Y., Zhao, J., Wang, X., Bennett, J., & Zhou, Z. (2010). Valuation of flood reductions in the Yellow River Basin under land use change. *J WATER RES PL-ASCE*, 136(1), 106-115.
- Remo, J., Pinter, N., & Heine, R. (2010). The use of retro- and scenario-modeling to assess effects of 100 + years river of engineering and land-cover change on Middle and Lower Mississippi River flood stages. *J HYDROL*, 376(3-4), 403-416.
- Schilling, K., Jha, M., Zhang, Y., Gassman, P., & Wolter, C. (2008). Impact of land use and land cover change on the water balance of a large agricultural watershed: Historical effects and future directions. *WATER RESOUR RES* 44, doi:10.1029/2007WR006644.
- Shiferaw Feleke, R. L. (2003). Determinants of Food Security in Southern Ethiopia . American Agricultural Economics Association Meetings in Montreal, Canada, 1-29.
- Tilahun A. & Robert D. (2006). Improved Decision-Making for Achieving Triple Benefits of Food Security, Income and Environmental Services through Modeling Cropping Systems in the Ethiopian Highlands. African Highlands Initiative (AHI) working paper no. 20.
- Tu, J. (2009). Combined impact of climate and land use changes on stream flow and water quality in eastern Massachusetts, USA. *J HYDROL*, 379, 268-283.

- Uloro Y. & Mengel K. (2014). Response of Enset (*Ensetventricosum* W.) to mineral fertilizers in southwest Ethiopia,. Sudanlage 35390 Giessen, Germany: Institute of Plant Nutrition of the Justus Liebig University.
- United States Department of Agriculture, Natural Resources Conservation Service (USDA-NRCS) (1986). "Urban Hydrology for Small Watersheds"; Technical Release 55, United States Department of Agriculture, Natural Resources Conservation Services, Conservation Engineering Division, Washington, DC, USA.
- Ward, P., Renssen, H., Aerts, J., van Balen, R., & Vandenberghe, J. (2008). Strong increases in flood frequency and discharge of the River Meuse over the late Holocene: impacts of long-term anthropogenic land use change and climate variability. *HYDROL EARTH SYST SC.*, 12(1), 159-175.
- Yimer, I. M. (2008). Effects of different land use types on infiltration capacity in a catchment in the highlands of Ethiopia. *Soil Use and Management*, 24, 344–349.
- Yirmaga, M. T. (2013). Improving the Indigenous Processing of Kocho, an Ethiopian Traditional Fermented Food. *Nutrition & Food Sciences*, 3(1), 1-6.
- Zehetner, F., & Miller, W. (2006). Erodibility and runoff-infiltration characteristics of volcanic ash soils along an altitudinal climosequence in the Ecuadorian Andes, *Catena*. *Catena*, 65, 201-213.
- Zeiger, M., & Fohrer, N. (2009). Impact of organic farming systems on runoff formation processes-A long-term sequential rainfall experiment, *Soil Till. Res. Soil Tillage*, 102, 45-54.

Figures

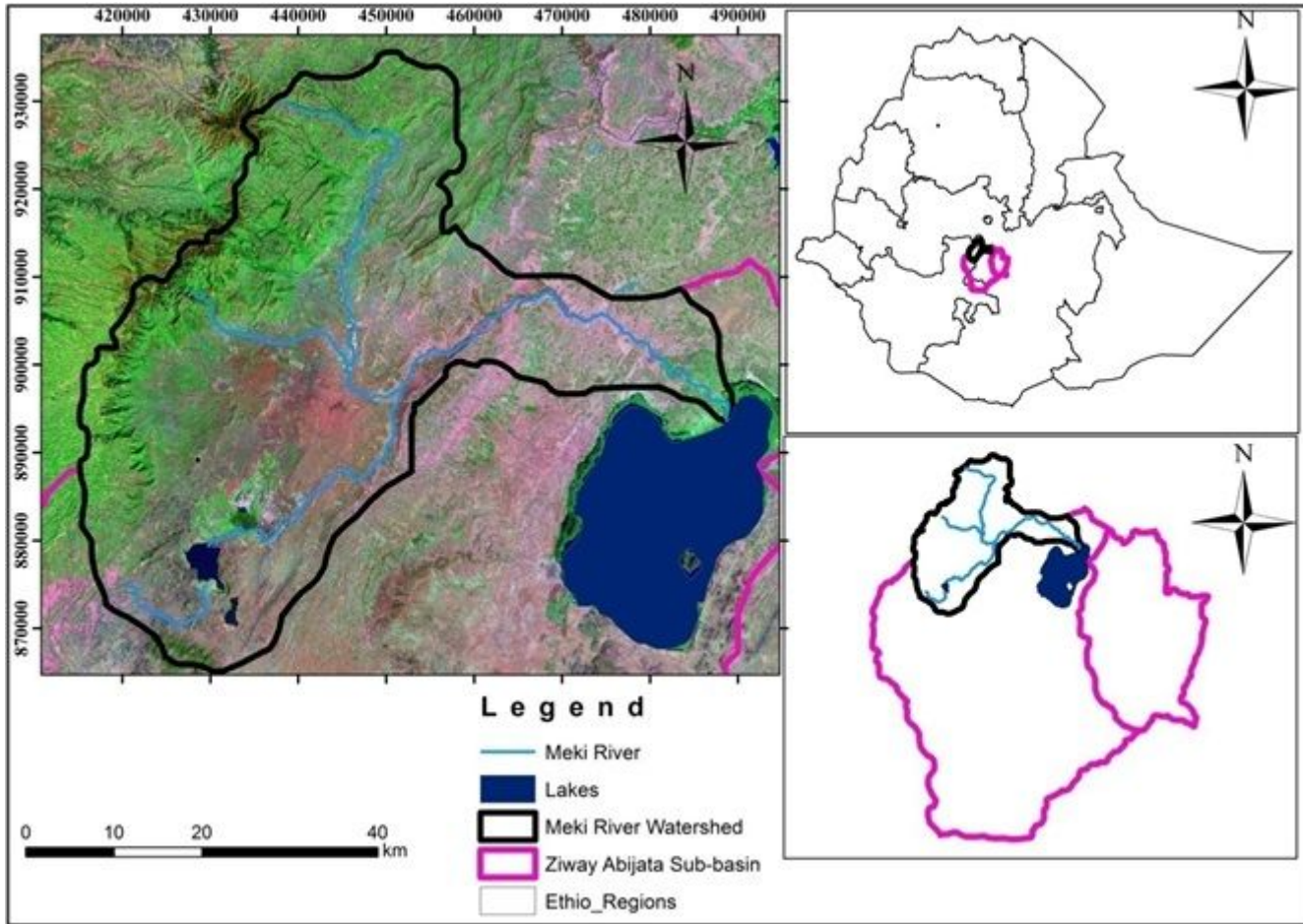


Figure 1

Study area map

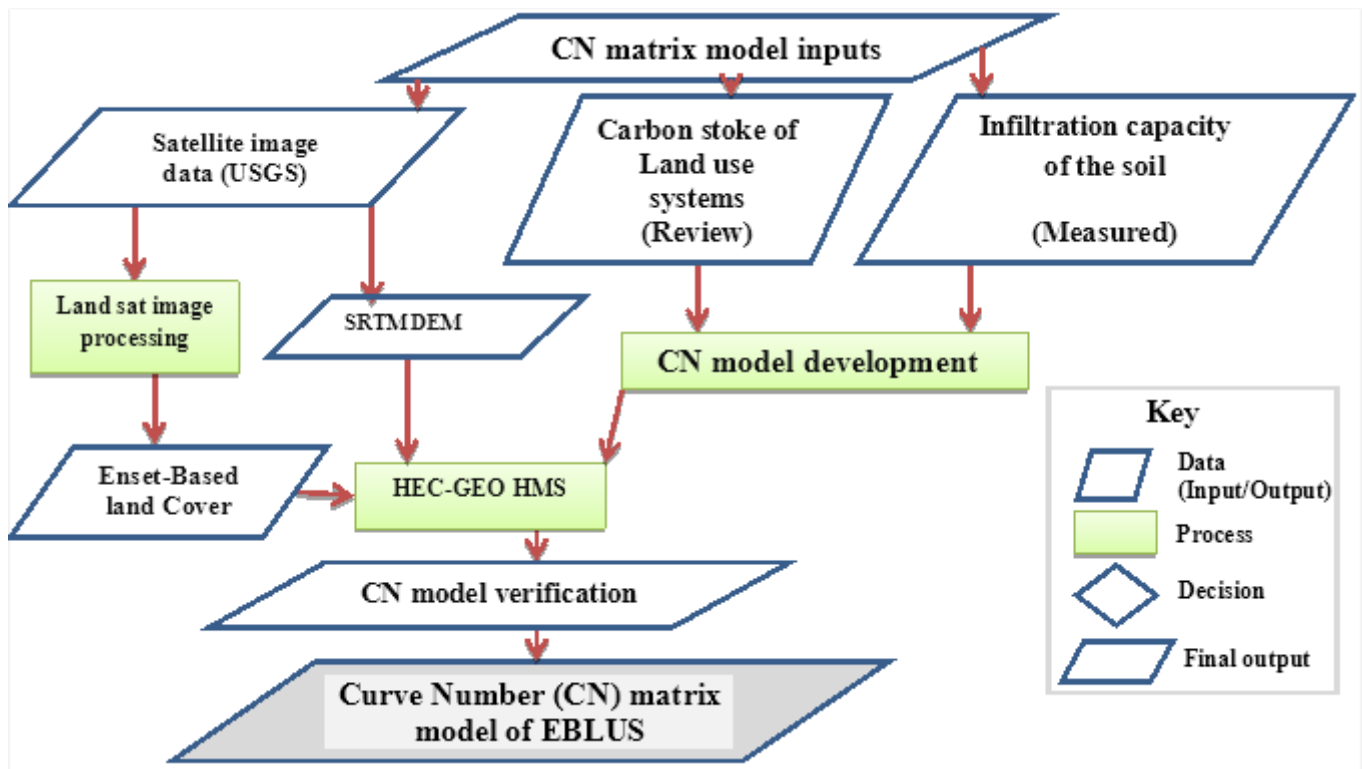


Figure 2

CN matrix model flow diagram

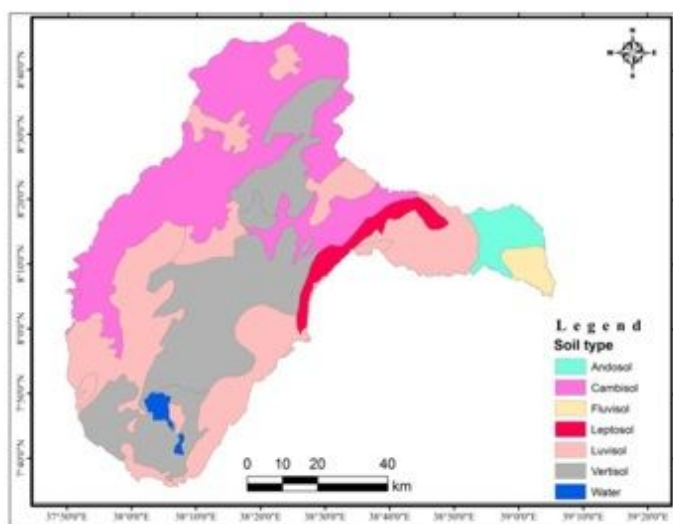
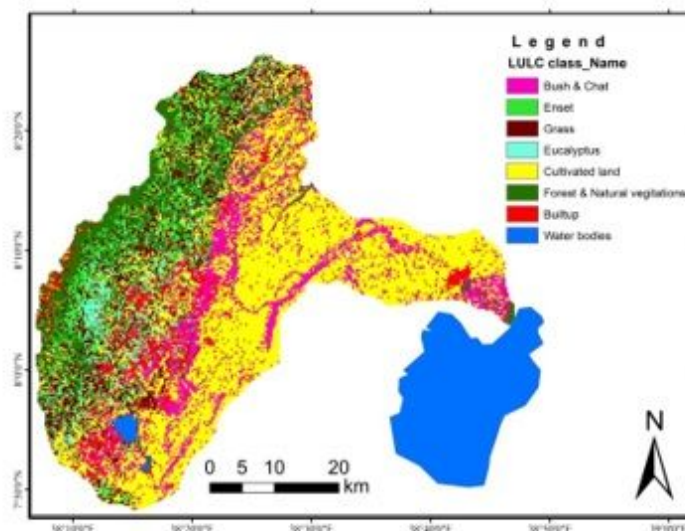
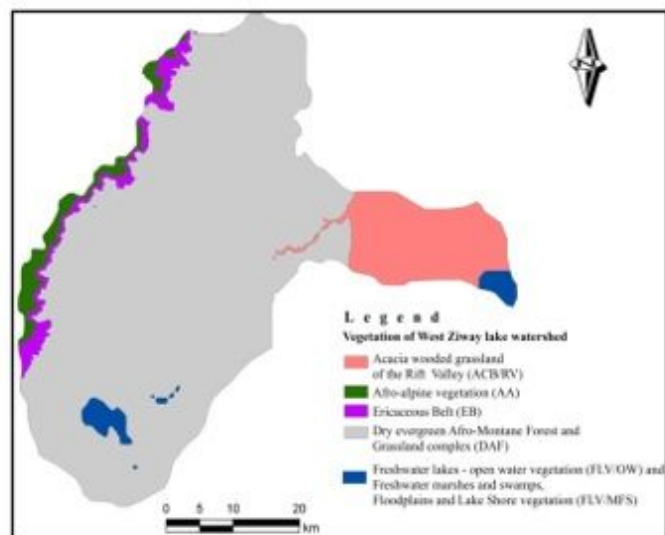


Figure 3

Dominant Vegetation zone, Land cover & soil type maps of the study area



Figure 4

Vegetation zone verification assessment A = Divide line at western end of the watershed where more than half part of the watershed is visible (Silti zone) B & F = Western upper part of Meskan woreda (Yewutin & Yetebon respectively) C = Found around Eastern Meskan woreda and Western Sodo woreda D = Scene at Chohamba Meskan woreda E = Conversion from lake to wetland (Lake Ziway)



Figure 5

Amozi-meter infiltration measurement of EBLUS

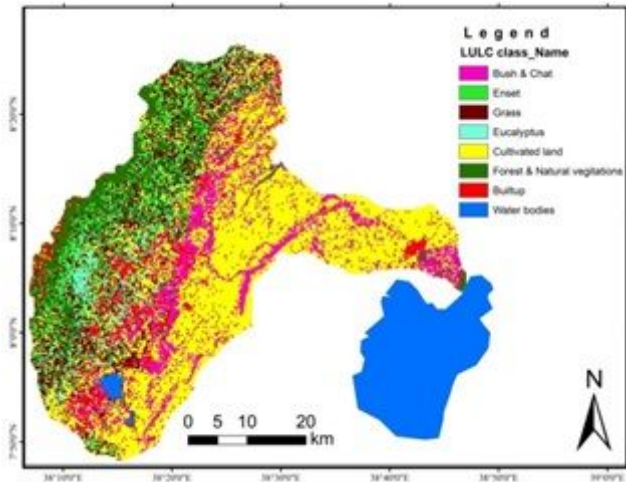


Figure 6

Land use system of the area for CN mapping

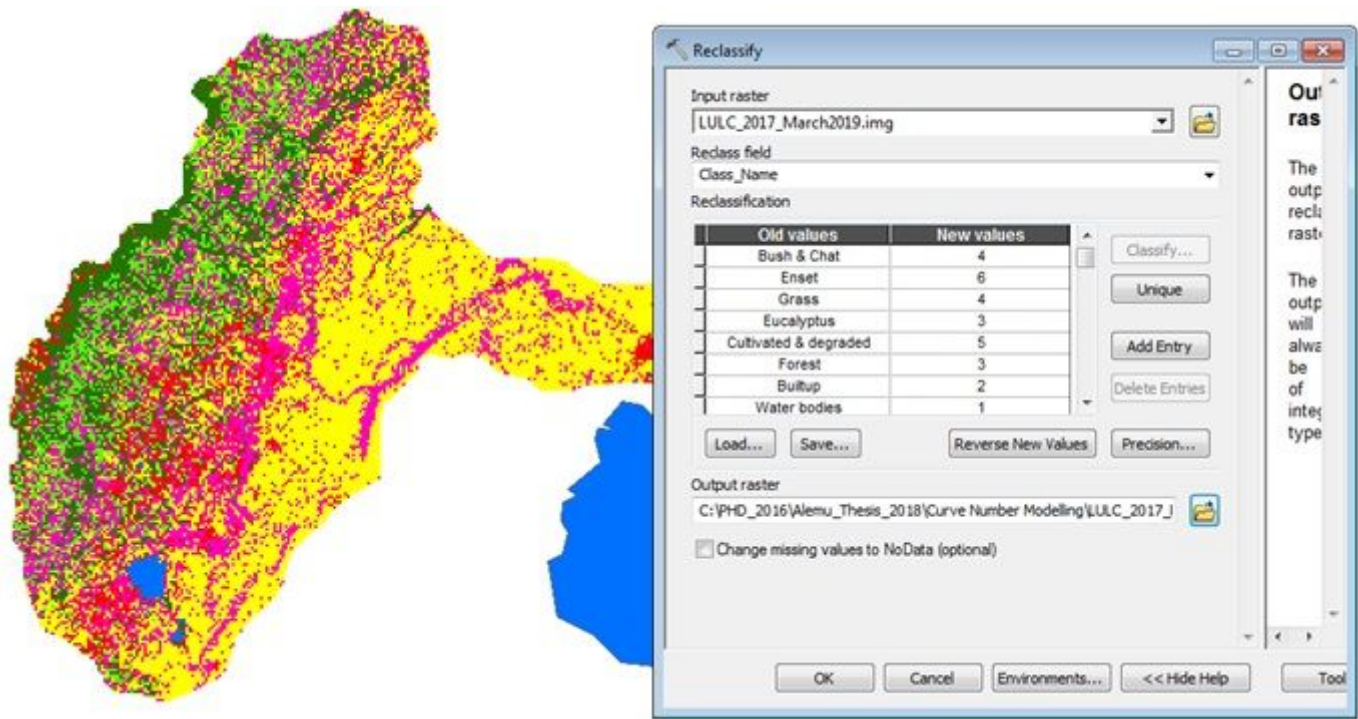


Figure 7

Reclassification window with assigned new values

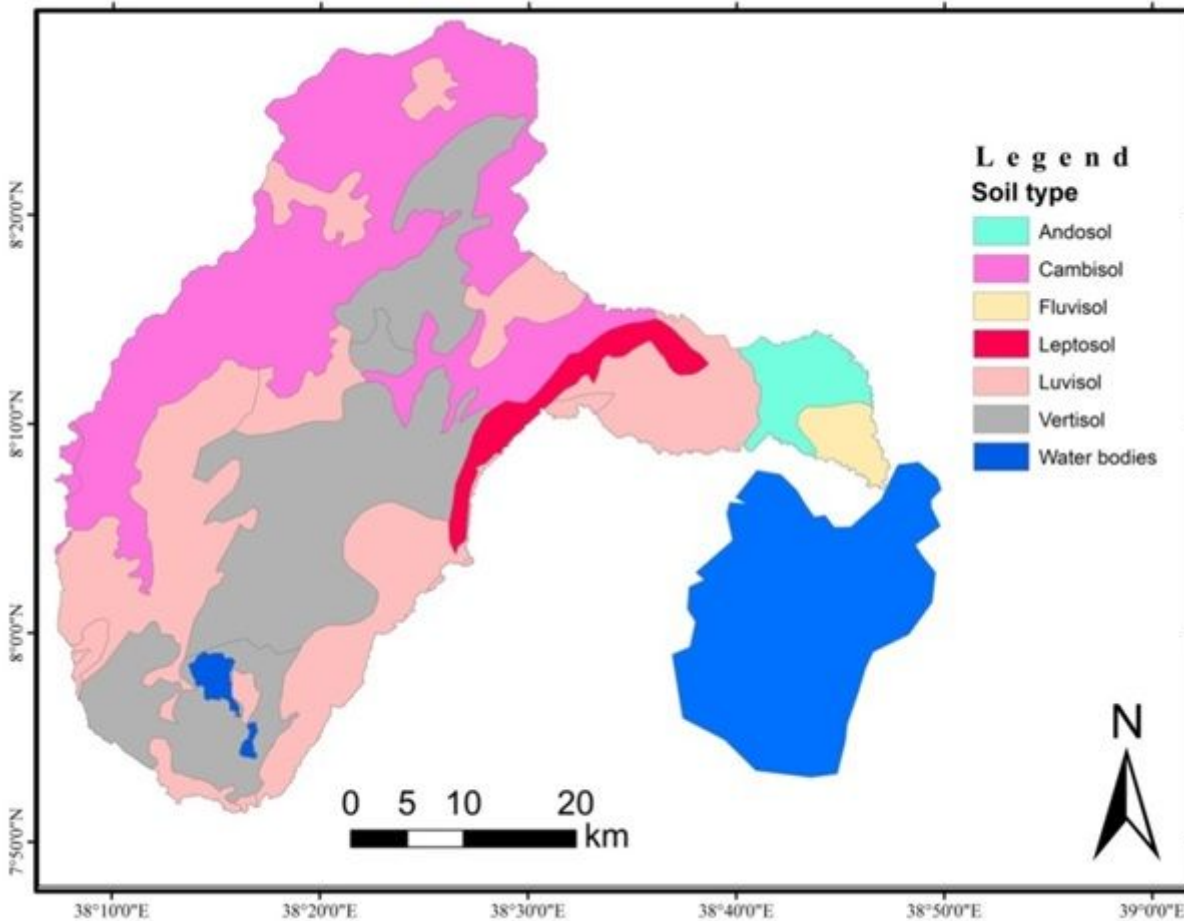


Figure 8

Soil map of the area (MWIE, 2017)

FID	Shape *	DIGS	DIGSOIL	soil	Area	Area_he	Tex	Soilmappi	Soil	Name	MU_GLO	Soil_WZ_201
6	Polygon	38	0	605	1022	102268.5	1	ANz 2/3 ab	B	Andosol	16903	
1	Polygon	8	0	604	108.	10831.52	3	CMe 3 de	B	Cambisol	16932	
5	Polygon	23	0	7	192.	19203.82	2	CMx 2/3 bc	B	Cambisol	16932	
15	Polygon	10	0	2	635.	63578.44	3	CMe 3 de	B	Cambisol	16964	
14	Polygon	21	0	24	139.	13999.45	1	FLc 1/2 ab	B	Fluvisol	16982	
2	Polygon	9	0	16	69.1	6910.35	3	LP 3 cd	C	Leptosol	16808	
0	Polygon	6	0	607	34.4	3448.9	3	LVh 1/2 cd	C	Luvisol	16739	
3	Polygon	11	0	17	735.	73572.59	2	LVh 1/2 bc	C	Luvisol	16739	
7	Polygon	40	0	6	7.53	752.85	3	LVh 1/2 de	C	Luvisol	16739	
8	Polygon	45	0	10	34.4	3448.04	3	LVh 1/2 de	C	Luvisol	16739	
9	Polygon	3	0	1	17.1	1716.35	2	LVh 1/2 bc	C	Luvisol	16739	
16	Polygon	28	0	11	1570	157018.4	3	LVh 1/2 de	C	Luvisol	16739	
17	Polygon	18	0	15	274.	27427.94	1	LVh 1/2 ab	C	Luvisol	16739	
18	Polygon	50	0	22	180.	18042.89	1	LVh 1/2 ab	C	Luvisol	16739	
19	Polygon	50	0	22	53.9	5391.7	2	LVh 1/2 c	C	Luvisol	16739	
22	Polygon	18	0	15	44.6	4463.49	1	LVh 1/2 ab	C	Luvisol	16739	
23	Polygon	5	0	4	50.2	5028.65	3	LVh 1/2 cd	C	Luvisol	16739	
4	Polygon	18	0	15	342.	34274.01	1	VRe 1 a	D	Vertisol	16851	
10	Polygon	5	0	4	131.	13131.2	2	VRe 1 bc	D	Vertisol	16855	
20	Polygon	50	0	22	683.	68333.52	2	VRe 1 bc	D	Vertisol	16839	
21	Polygon	18	0	15	17.5	1755.23	1	VRe 1 a	D	Vertisol	16851	
11	Polygon	0	0	Wat	2.83	282.53	0		0	Water	16994	
12	Polygon	0	0	Wat	0.1	9.59	0		0	Water	16994	
13	Polygon	0	0	Wat	13.2	1324.4	0		0	Water	16994	

Figure 9

Hydrologic soil group (HSG) assignment

soil	Area	Area_he	Tex	Soilmappi	Soil	Name	MU_GLO	Soil_WZ_2018_1.HYDROID	Soil_WZ_2018_1.PctA	Soil_WZ_2018_1.PctB	Soil_WZ_2018_1.PctC	Soil_WZ_2018_1.PctD
2	635.	63578.44	3	CMe 3 de	B	Cambisol	16964	16	0	100	0	0
24	139.	13999.45	1	FLc 1/2 ab	B	Fluvisol	16982	15	0	100	0	0
16	69.1	6910.35	3	LP 3 cd	C	Leptosol	16808	3	0	0	100	0
607	34.4	3448.9	3	LVh 1/2 cd	C	Luvisol	16739	1	0	0	100	0
17	735.	73572.59	2	LVh 1/2 bc	C	Luvisol	16739	4	0	0	100	0
6	7.53	752.85	3	LVh 1/2 de	C	Luvisol	16739	8	0	0	100	0
10	34.4	3448.04	3	LVh 1/2 de	C	Luvisol	16739	9	0	0	100	0
1	17.1	1716.35	2	LVh 1/2 bc	C	Luvisol	16739	10	0	0	100	0
11	1570	157018.4	3	LVh 1/2 de	C	Luvisol	16739	17	0	0	100	0
15	274.	27427.94	1	LVh 1/2 ab	C	Luvisol	16739	18	0	0	100	0
22	180.	18042.89	1	LVh 1/2 ab	C	Luvisol	16739	19	0	0	100	0
22	53.9	5391.7	2	LVh 1/2 c	C	Luvisol	16739	20	0	0	100	0
15	44.6	4463.49	1	LVh 1/2 ab	C	Luvisol	16739	23	0	0	100	0
4	50.2	5028.65	3	LVh 1/2 cd	C	Luvisol	16739	24	0	0	100	0
15	342.	34274.01	1	VRe 1 a	D	Vertisol	16851	5	0	0	0	100
4	131.	13131.2	2	VRe 1 bc	D	Vertisol	16855	11	0	0	0	100
22	683.	68333.52	2	VRe 1 bc	D	Vertisol	16839	21	0	0	0	100
15	17.5	1755.23	1	VRe 1 a	D	Vertisol	16851	22	0	0	0	100
Wat	2.83	282.53	0		0	Water	16994	12	0	0	100	0
Wat	0.1	9.59	0		0	Water	16994	13	0	0	100	0
Wat	13.2	1324.4	0		0	Water	16994	14	0	0	100	0

Figure 10

Standard curve number matrix assignment for different soil groups

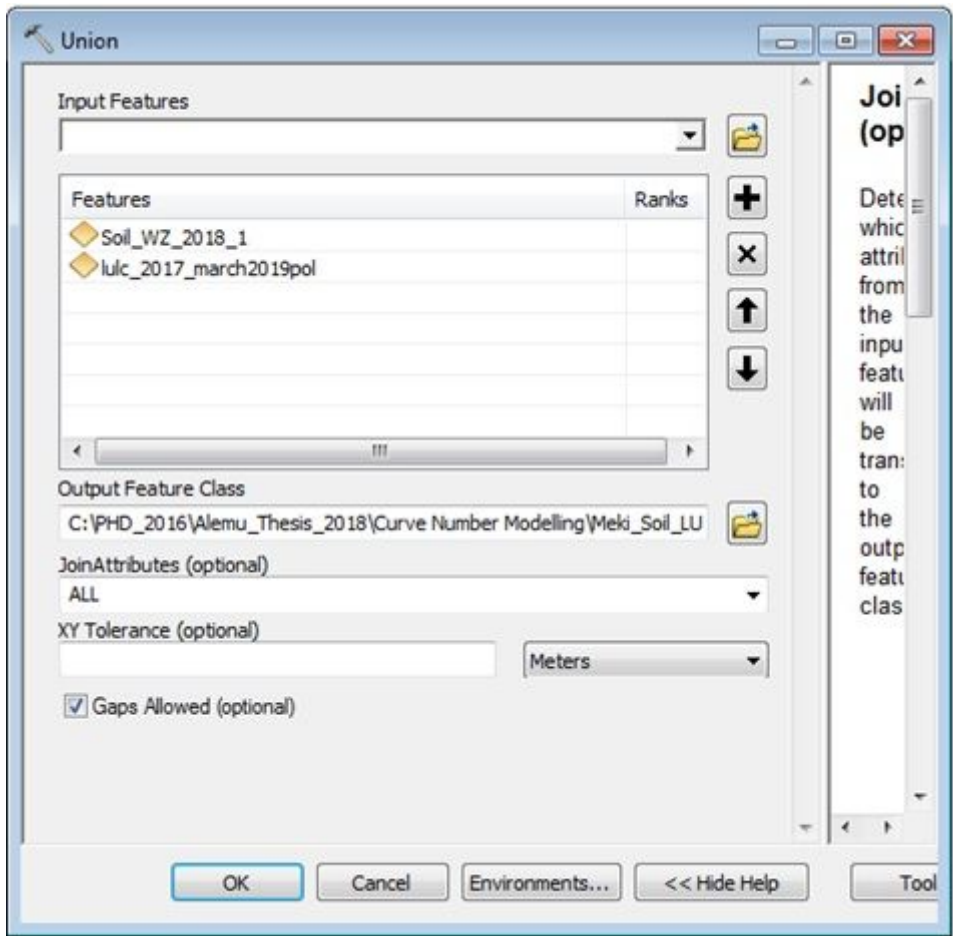


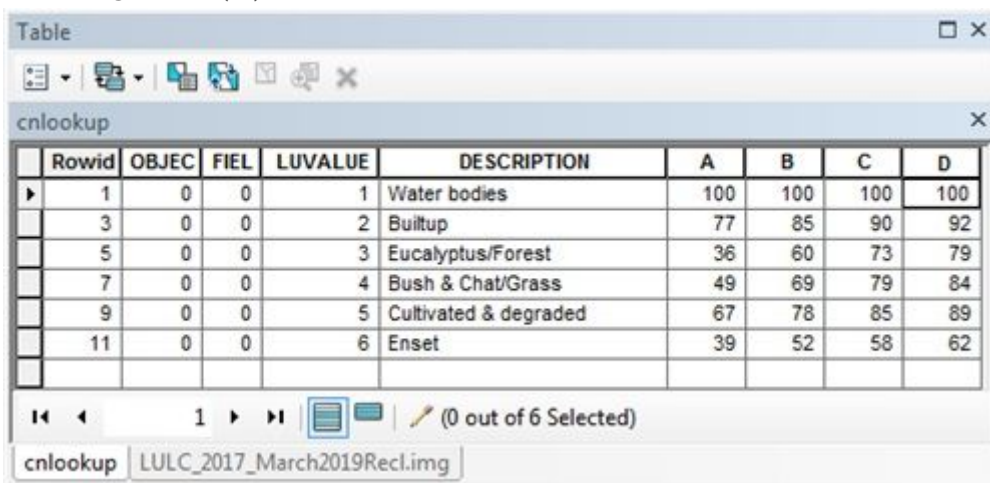
Figure 11

Soil land use union (Merge) of the watershed

FID	Shape	FID_lulc	ID	GRID	Value	FID_Soil_W	DIG	DIGS	soil	Are	Are	Text	Soilm	Name	MU_G	HSG	HYDROID	PctA	PctB	PctC	PctD
0	Polygon	0	1	5	5	-1	0	0		0	0	0			0		0	0	0	0	0
1	Polygon	1	2	4	4	-1	0	0		0	0	0			0		0	0	0	0	0
2	Polygon	2	3	6	6	-1	0	0		0	0	0			0		0	0	0	0	0
3	Polygon	4	5	3	3	-1	0	0		0	0	0			0		0	0	0	0	0
4	Polygon	6	7	5	5	-1	0	0		0	0	0			0		0	0	0	0	0
5	Polygon	7	8	4	4	-1	0	0		0	0	0			0		0	0	0	0	0
6	Polygon	10	11	5	5	-1	0	0		0	0	0			0		0	0	0	0	0
7	Polygon	11	12	4	4	-1	0	0		0	0	0			0		0	0	0	0	0
8	Polygon	14	15	3	3	-1	0	0		0	0	0			0		0	0	0	0	0
9	Polygon	15	16	4	4	-1	0	0		0	0	0			0		0	0	0	0	0
1	Polygon	16	17	5	5	-1	0	0		0	0	0			0		0	0	0	0	0
1	Polygon	19	20	3	3	-1	0	0		0	0	0			0		0	0	0	0	0
1	Polygon	22	23	6	6	-1	0	0		0	0	0			0		0	0	0	0	0
1	Polygon	23	24	4	4	-1	0	0		0	0	0			0		0	0	0	0	0
1	Polygon	24	25	5	5	-1	0	0		0	0	0			0		0	0	0	0	0
1	Polygon	25	26	4	4	-1	0	0		0	0	0			0		0	0	0	0	0
1	Polygon	32	33	6	6	-1	0	0		0	0	0			0		0	0	0	0	0
1	Polygon	33	34	5	5	-1	0	0		0	0	0			0		0	0	0	0	0
1	Polygon	46	47	6	6	-1	0	0		0	0	0			0		0	0	0	0	0
1	Polygon	47	48	4	4	-1	0	0		0	0	0			0		0	0	0	0	0
2	Polygon	48	49	3	3	-1	0	0		0	0	0			0		0	0	0	0	0
2	Polygon	49	50	5	5	-1	0	0		0	0	0			0		0	0	0	0	0

Figure 12

Avoiding sliver (-1) of the soil land use union of the watershed



Rowid	OBJEC	FIEL	LUVALUE	DESCRIPTION	A	B	C	D
1	0	0	1	Water bodies	100	100	100	100
3	0	0	2	Builtup	77	85	90	92
5	0	0	3	Eucalyptus/Forest	36	60	73	79
7	0	0	4	Bush & Chat/Grass	49	69	79	84
9	0	0	5	Cultivated & degraded	67	78	85	89
11	0	0	6	Enset	39	52	58	62

Figure 13

Lookup table considering EBLUS

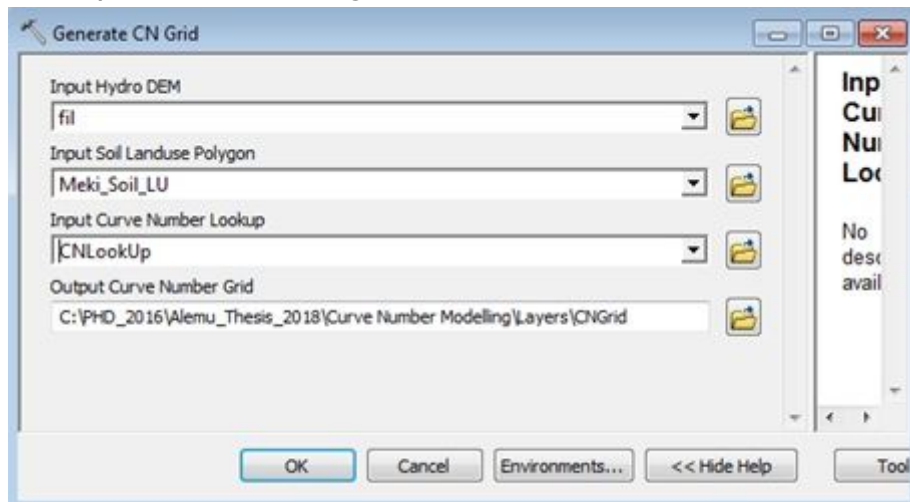


Figure 14

CN generation considering Enset-Based land use system

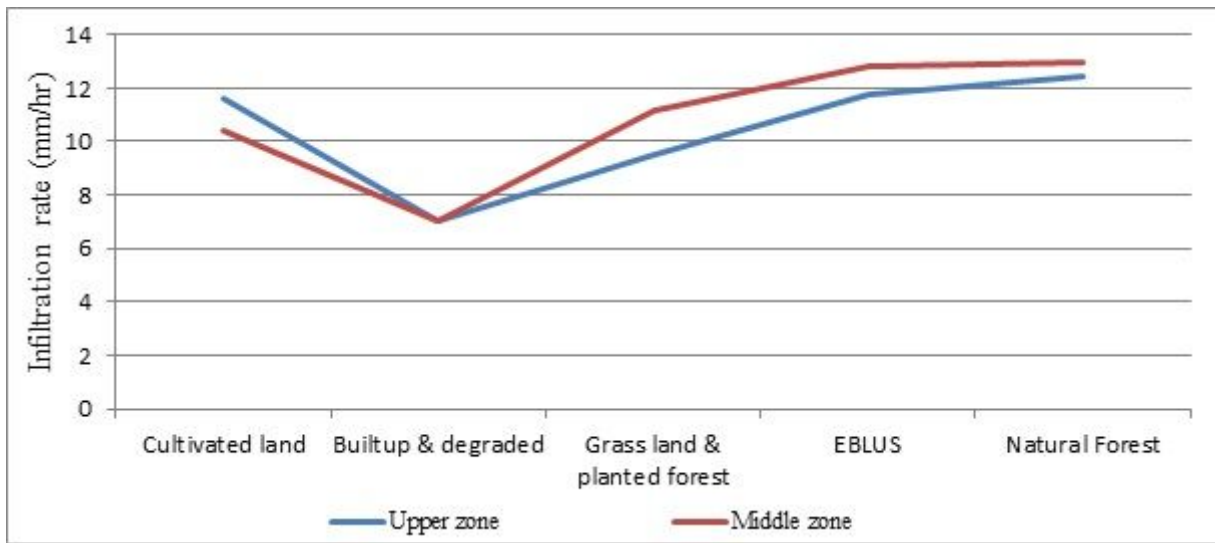


Figure 15

Vegetation zone based infiltration capacity of the soil (mm/hr)

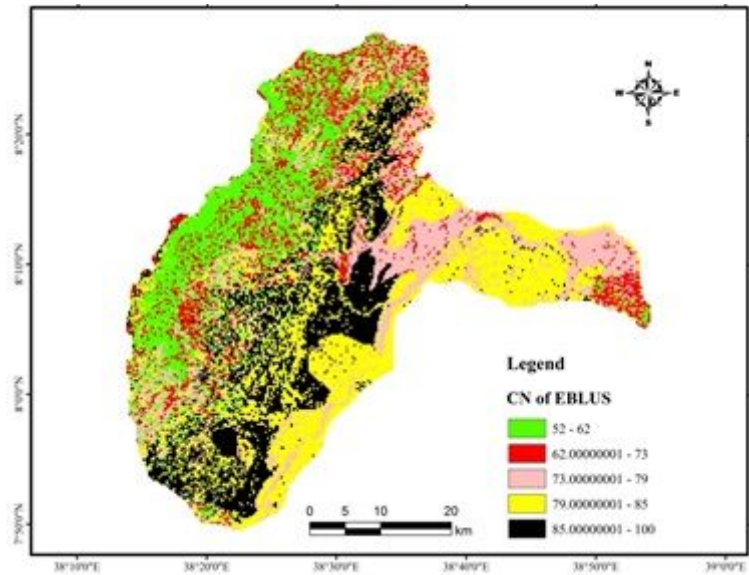


Figure 16

Average soil loss from sub-watersheds with respect to Rift valley limit

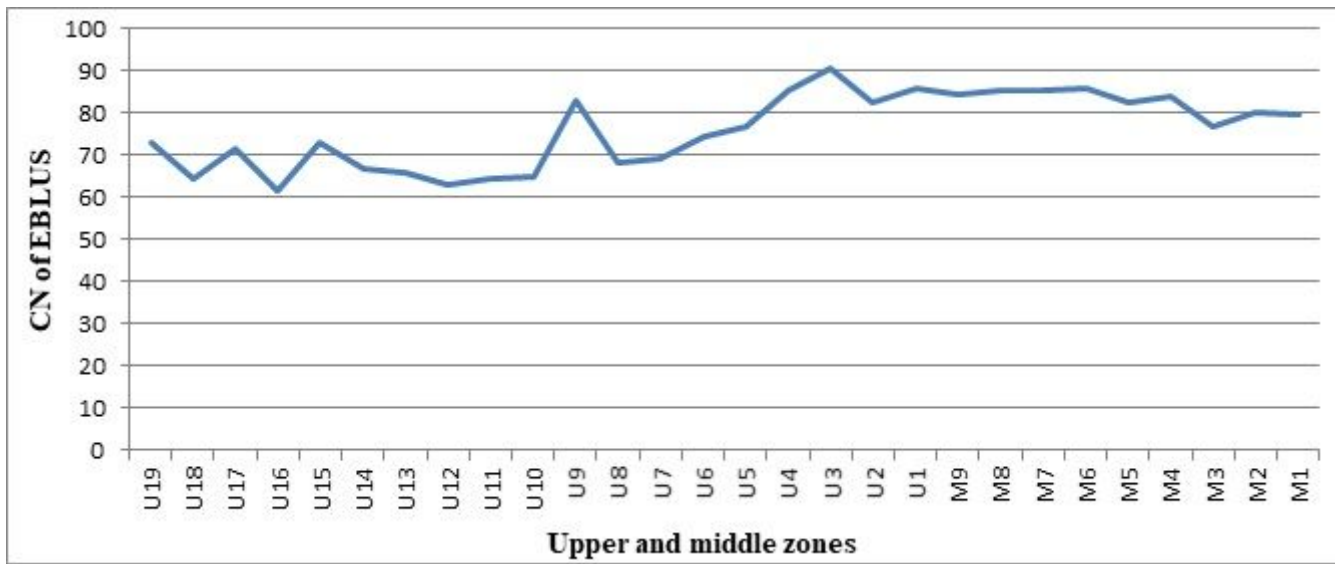


Figure 17

Curve number of EBLUS in the upper and middle zones

Supplementary Files

This is a list of supplementary files associated with this preprint. Click to download.

- [Supplementary.docx](#)